R & M No. 3824

R &M No. 3824

PROCUREMENT EXECUTIVE, MINISTRY OF DEFENCE

Aeronautical Research Council
Reports and Memoranda

THE DEVELOPMENT OF A PARAMETRIC METHOD OF MEASURING FIN FATIGUE LOADS BASED ON FLIGHT MEASUREMENTS ON A LIGHTNING Mk.T5

by

Anne Burns, B.A.,
J.P. Thompson, M.Sc.,
and E.W. Wells

Structures Department, RAE Farnborough, Hants

London: Her Majesty's Stationery Office
1978

PRICE £6 NET

THE DEVELOPMENT OF A PARAMETRIC METHOD OF MEASURING FIN FATIGUE LOADS BASED ON FLIGHT MEASUREMENTS ON A LIGHTNING MK T5

By Anne Burns, BA, J. P. Thompson, MSc and E. W. Wells

Reports and Memoranda No 3824*
December 1976

SUMMARY

The Report discusses briefly the philosophy of parametric methods of load measurement in which load is not measured directly, but is deduced from a statistical correlation with an appropriate combination of aircraft motion variables and control surface angles. It describes a full-scale flight experiment on a Lightning Mk T5 aimed at developing a parametric method for the measurement of fin fatigue loads under operational conditions. An empirical relationship is established between the fin root bending moment, as determined from a multi-strain gauge installation, and a combination of parameters. The parameters from which the combination is selected include translational and rotational accelerations, rates of rotation, rudder angle and angle of sideslip. The study covers the measurement of fin loads under a wide range of loading conditions.

* Replaces RAE Technical Report 76161, ARC 37442

CONTENTS

1 INTRODUCTION

The term parametric method of load measurement is used in this Report to describe a method of obtaining information on the occurrences of structural loads for fatigue purposes which is based on flight measurements of certain key parameters rather than on multi-strain measurements. The parameters in mind are those that relate to loading actions or to overall responses of the aircraft. The principle behind the parametric method is not new; as long ago as the early 1950s, a single parameter, normal acceleration at the CG, was widely used to obtain information on fatigue loads in the wings of fixed-wing aircraft. Attention was focussed on the wing, since experience at that time indicated this to be the critical component. However, by the late 1960s fatigue failures in other parts of the structure, particularly the fin were becoming prevalent, pointing to the necessity for the development of a fatigue monitoring system applicable to general structural components rather than for the wing alone. It was against this background that the experimental study described in this Report was undertaken.

There are several reasons for adopting a parametric method for load data collection under operational conditions rather than the more direct method based on multi-strain measurements which is commonly used for load determination on prototype aircraft and in special investigations. (Pressure plotting supplemented by acceleration measurements is not considered a serious contender for operational use.) First and foremost, the sensors for the parametric method are easier to install and calibrate - calibration can often be carried out remotely as opposed to the strain gauge installation which is best calibrated *in situ* by the application of loads. Maintenance is easier and, should the sensors become unserviceable, they can be replaced much more readily than can strain gauges. Many of the required sensors are well proven in service and some may even be a standard fitment for other purposes, e.g. accident recording. Secondly, there is the wider consideration that parametric data, because of their basic form, can be more useful than strain data for building up generalised fatigue spectra and even for updating structural design criteria relating to limit loads. Parametric data is also of more use in identifying loading actions which are particularly damaging in fatigue, should any such occur, thus enabling the operator to exercise some control over fatigue life consumption. These latter potentialities can only be realised in a multi-parametric method if data on individual parameters are extracted separately.

To study the application of parametric methods to fin loads in fighter type aircraft, an experiment was mounted on a Lightning Mk.T5 (Fig.1) in which overall loads were measured near the fin root by means of a multi-strain gauge installation, using the Skopinski[1] method to optimise the derivation of load from the measured strains. At the same time measurements were made of a number of parameters describing the motions of the aircraft, the deflections of the relevant control surfaces and the angle of sideslip. Because of instrumental limitations only a selection of the strain gauges and parameters could be recorded simultaneously, with the result that the measurements are not as comprehensive as could have been wished. Measurements were taken under a wide spectrum of loading conditions including flight refuelling and carriage of symmetric and asymmetric wing stores. The flight programme included manoeuvres intended to be representative of Service practice as well as simpler manoeuvres based on design cases, each of which emphasised a particular way of loading the fin. Manoeuvres were performed both with and without yaw and roll autostabilisation. The Report presents an account of the parametric method developed and its application to the Lightning fin loads. Emphasis is placed on fin root bending moment since past experience has shown that fatigue problems in the main structure of aerofoils are usually associated with tensile strain arising from bending moment, and that the root section is likely to be critical largely because of the presence of joints in what is usually a highly stressed part of the structure.

2 BASIC CONCEPTS

Before proceeding further it is proposed to discuss briefly some of the concepts that underlie the approach adopted in this Report. Further background information on the potentialities of parametric methods for predicting service lives of military aircraft and helicopters can be found in recent reports by Hovell[2] and by Hovell and Sturgeon[3].

2.1 The parameter - load relation

The crux of the problem of using parametric methods for assessing fatigue loads lies in the interpretation of the parametric data in terms of the required load spectra. Two radically different lines of approach to this problem can be distinguished; in the first, the parametric data are used solely to identify the flight condition, and the load spectra associated with these conditions calculated from deterministic equations. In the second, structural load spectra are

deduced directly from the parametric data by means of an empirical relationship determined statistically from special flight measurements. The deterministic equations if sufficiently simplified might be expected to approximate to the empirical relation, but whether such drastic simplification is feasible has yet to be proven. In the meantime the empirical approach provides a powerful means of effecting the simplification necessary for a successful operational method, and it is this approach which is fundamental to the method of this Report.

2.2 The consideration of time history

Operational data, gathered for fatigue purposes are almost inevitably, by virtue of their quantity, reduced at some stage in their collection to a form of distributional counts - whether it be cumulative distributions of levels exceeded, distributions of peaks and troughs or some form of range count. It follows that, in order to relate parametric data to load data for fatigue purposes it is unnecessary for their time histories to be similar; all that is required is that a consistent relation should exist between the respective sets of counts[4]. Nevertheless in developing a parametric method it was decided not to throw away all consideration of time history for two reasons:-

(i) Because of the complexity of dealing with a number of parameters without considering their relative time histories.

(ii) Because similarity in the time histories of the parametric representation and of the required load itself engenders confidence in the validity of the parametric representation for future use when the spectrum of flight conditions may be widened.

The second reason implies a decision to aim at a combination of parameters with a close time history to that of the required load.

In the initial stages of the Lightning analysis, correlation of parameters with loads was studied at all instants of time. This procedure proved too cumbersome and did not readily lead to optimising the choice of parameters. A method was therefore devised whereby a combination of instantaneous values of the parameters was sought which possessed a similar time history to that of the load only inasmuch as all peaks and troughs, of significance in fatigue, tended to coincide in time and to be matched in magnitude. At a later stage consideration was given to the matching of the time histories between matched points mainly to ensure that the parametric combination did not produce superfluous peaks and troughs.

2.3 The treatment of structural oscillatory loads

In the smaller military type aircraft, structural oscillations associated with flexibility are not likely to play such a prominent part in producing internal loads as in the larger flexible aircraft. Nevertheless some consideration may have to be given to this type of loading since it can produce significant fatigue damage particularly in the case of strike aircraft subjected to low level turbulence. Structural oscillations during buffetting, in high angle of attack manoeuvres, can also contribute significantly to fatigue damage. In the case of the Lightning, significant oscillations occurred at the fin only during low level flight in turbulence.

Judging from experience with the Lightning where the dominant fin oscillation at 8.6Hz was most marked at the aft end, structural oscillatory loading in fins is likely to vary markedly with locality, and for this reason does not lend itself readily to parametric representation. Moreover the inclusion of frequencies high enough to cover structural oscillations leads to difficulties owing to the varying phase shifts in the signals from different types of sensors. It was therefore decided to confine the parametric method to a waveband whose upper limit was high enough to cover rigid body frequencies only and to leave the treatment of structural oscillatory loading to a later stage when dynamic factors appropriate to the locality could be introduced as necessary. The magnitude of such factors and indeed the need to include them at all, could then be assessed in the light both of the oscillatory content of the special flight test measurements on which the parametric formula was based and of the operation frequency of occurrence of the particular flight conditions giving rise to the oscillatory loads. Where a particular part of the structure was in question a limited quantity of operational data in which the parametric method was supplemented by the use of a counting strain gauge or fatigue sensor could be used to produce a good estimate of the dynamic factor. The former was preferable in that it allowed greater refinement in the association of dynamic factors with particular loading cases, and gave greater accuracy when the quantity of data was small.

2.4 The conditioning of parameters

Some adjustments of the parametric values on which the parametric combination is to be based may have to be made if the part of the load attributable to each parameter is to vary linearly, at least to a first approximation, with

that parameter. (Linearity is desirable since it facilitates both the optimisation of the parametric combination and the process of operational data reduction.) The adjustments in mind are those that arise from simple theoretical considerations; they relate to the flight conditions pertaining at the time, and involve quantities such as dynamic pressure, true air speed, Mach number and aircraft mass. Under operational conditions, such adjustments would preferably be made instrumentally, prior to recording, although they could be made later as part of the data reduction process. In either case such conditioning is a complication to be avoided, if at all possible, by a choice of parameters which require no adjustment or so little that it can be neglected. In this respect, the parameter acceleration, whether linear or rotational, may have some advantage over other parameters such as rotational rates of motion, angle of sideslip and control surface angles, all of which require extensive scaling according to dynamic pressure, while rate parameters require further scaling according to the inverse of true air speed. Acceleration on the other hand mainly requires scaling according to changes in aircraft mass which may well be small enough for their effect to be neglected or allowed for in a crude manner, for example by the introduction of a 'mission' factor when heavy stores are carried. Although for tailplanes the relation between normal acceleration and load may be strongly dependent on Mach number[5], for fins the dependence is expected to be less. Conditioning with Mach number, both as regards acceleration and other parameters, was omitted in the Lightning study although some attention was given to the difference between the subsonic and supersonic relationship of acceleration to load.

3 METHOD OF DERIVING PARAMETRIC FORMULA

3.1 Outline of method

The method developed for determining a combination of parameters to give information on the overall loads, i.e. bending moment, shear and torque at a structural cross-section is now outlined briefly, followed by a more detailed account of the application to the Lightning fin root bending moment.

Starting from the point where flight measurements covering a comprehensive set of flight loading conditions are available in the form of time histories of the relevant parameters and strain gauges the procedure is as follows:-

(i) Combine the strain gauge signals in the appropriate proportions according to Skopinski's method[1] to give the time histories of the required overall load; the variation of Skopinski's method developed by

Hovell, Webber and Roberts[6] may be useful here. Apply a constant correction if necessary such that the combination produces zero load in straight and level flight. (Lateral trimming loads on the fin and rudder are assumed to be insignificant throughout the flight range.)

(ii) Filter out all structural frequencies from the parameters and from the overall load by application of a low pass filter.

(iii) Perform any differentiation required (signals from rate gyros may have to be differentiated to give rotational accelerations.)

(iv) Select maxima and minima values of the overall load together with simultaneous values of the parameters.

(v) Adjust these values of the parameters as required according to dynamic pressure, true air speed, Mach number and aircraft mass.

(vi) Run special regression analysis programme on above data to select parameters and optimise their linear combination to give overall load[7].

(vii) Make final choice of parametric combination, re-running programme if necessary to include subjectively chosen parameters.

(viii) Check final choice to ensure close correlation between time histories of overall load and parametric combination outside matched points.

3.2 Choice of parameters

The choice under (vii) is guided by the following considerations:-

(i) The advantages of trading off accuracy for simplicity by reducing the number of parameters.

(ii) The preference for parameters requiring little or no adjustment for flight conditions.

(iii) The preference for parameters which can be measured easily and with a high degree of reliability. Consistency of sensor performance, freedom from noise, and linearity of calibration are among the factors to be looked for here.

(iv) The preference for parameters which provide data useful for other purposes (see introduction).

4 APPLICATION OF PARAMETRIC METHOD TO LIGHTNING FIN LOADS

4.1 Determination of fin root loads from measured strains

It is not proposed to describe in detail the application of the Skopinski method to the determination of the Lightning fin loads. Some references to the special strain gauge calibration tests will be found in Appendix A and the types and positions of the strain gauge bridges are shown in Fig.2. The final combinations of strain signals chosen for determining overall loads at the fin root were as follows:-

$$BM_{root} = -8.78\varepsilon_{b_2} + 28.79\varepsilon_{b_3} + 31.77\varepsilon_{b_4} \quad (1)$$

$$S_{root} = 4.93\varepsilon_{S_2} + 7.12\varepsilon_{S_3} + 5.81\varepsilon_{S_4} + 6.71\varepsilon_{S_5} + 5.52\varepsilon_{S_{rsw}} + 19.59\varepsilon_{b_2} \quad . \quad (2)$$

No combination is given for torque since, of those obtained, none appeared likely to prove reliable when applied to flight load measurements owing to a tendency to derive torque as a small difference of two large quantities. The shear combination was used only in a supplementary study of the variation in spanwise load centre, the results of which are given in Appendix B. Some indications of the variation in chordwise distribution of the root bending moment and shear load is also given in this Appendix.

In order to save time during the initial stages of the parametric analysis, the combination for fin root bending moment was reduced to a single strain gauge bridge signal as follows:-

$$BM_{root} = 53.32\varepsilon_{b_3} \quad . \quad (3)$$

Subsequent comparison with the bending moment obtained from the full combination (equation (1)) showed the difference to be small in comparison with the scatter in the parametric representation (see Fig.4), and the reduced combination was used throughout the parametric study. Results given in Appendix B are, however, based on the full combination.

4.2 Development of the relationship between fin root bending moment and flight parameters

The parameters in question were lateral acceleration at the fin ($\ddot{y}_f$), lateral acceleration at a point on the spine ($\ddot{y}_s$) *, yaw rate ($\dot{\psi}$), yaw

* The term lateral acceleration is used throughout the Report to denote lateral acceleration uncorrected for gravity effects due to changes in roll attitude, i.e. to denote acceleration as sensed by a lateral accelerometer mounted rigidly in the aircraft.

acceleration ($\ddot{\psi}$), roll rate ($\dot{\phi}$), roll acceleration ($\ddot{\phi}$), angle of sideslip at the airstream direction sensor nose station (β) and rudder angle (ζ). The latter was measured on only a limited number of flights, mainly supersonic, because of the limitation on the number of channels that could be recorded on the main recorder, and hence had to have separate treatment. Sensor positions are shown in Figs.1 and 3.

The recorded information on FM analogue tapes was digitised by a Hewlett-Packard Fourier analyser. At first, relationships were explored in a tentative way by calculation of correlations, to find which parameters appeared to be most significant. A relationship was then sought of the form

$$\text{fin root bending moment} = \sum a_n P_n \quad , \tag{4}$$

where the a_n were coefficients to be found and the P_n were the flight parameters. Roll and yaw rate, angle of sideslip and rudder angle were conditioned by multiplying by dynamic pressure and in the case of the first two parameters, by dividing by true air speed. The dynamic pressure q is the difference between total and static pressures, $(p_{tot} - p_s)$,

where
$$p_{tot} = p_s\left[1 + \frac{\gamma - 1}{2} M^2\right]^{\frac{\gamma}{\gamma-1}} \quad . \tag{5}$$

No adjustment was made to the accelerations to allow for variation in aircraft mass; the variation which was due to consumption of fuel and carriage of stores did not greatly affect the relevant inertias. Frequencies above 1Hz were filtered out of the data to remove the effect of structural oscillations. The data used referred to the following manoeuvres:-

rolling pull-outs, aileron rolls, yawing - with and without roll suppressed; aileron rolls, sideslips and a stretch of turbulence - all at subsonic speeds,

and also:-

missile break-away manoeuvres, rolls of various types, rudder kicks - all initiated at supersonic speeds.

Further details of these manoeuvres and loading cases are listed in Table 1.

For each manoeuvre maxima and minima of the output strain gauge bridge B_3, representing fin root bending moment (see Fig.4), were taken, together with the simultaneous values of the flight parameters listed earlier. All the computation up to this point was done on the Fourier analyser. The resulting data are listed in Table 2.

The required relation was sought from this data by means of a general multiple regression programme run on an ICL 1906S. The mode of operation of this programme was to find the best linear combination of the given flight parameters to represent the fin root bending moment, then to drop the least significant parameter and find a new combination of the remainder to represent fin root bending moment, and to continue this process till only one flight parameter was left. This process did not guarantee that at each stage the best combination of a given number of parameters was selected. Because of the intercorrelation between the parameters, it was found that parameters previously discarded could on occasion be reintroduced with advantage, particularly when the parametric formula was reduced to one or two parameters.

The first parameter to be discarded was $\ddot{\psi}$ which seemed reasonable since it might be expected to duplicate the combined presence of $\ddot{y}_s$ and $\ddot{y}_f$. Next was $\dot{\psi}$ suggesting that damping in yaw did not contribute significantly - the elimination of these yawing parameters produced no significant difference in the accuracy of the parametric formula (see regression run 1 of Table 3). β was discarded next, probably on the score of redundancy - it was quite closely correlated with both $\ddot{y}_s$ and $\ddot{y}_f$. The elimination of β did, however, cause a very slight drop in accuracy. This left $\dot{\phi}$ and the three accelerations $\ddot{\phi}$, $\ddot{y}_s$ and $\ddot{y}_f$. At this stage further elimination caused the accuracy to fall off ever more rapidly, suggesting that if the instrumentation could be accommodated operationally, this would be the best parametric formula for the Lightning. $\dot{\phi}$ was the next parameter to be discarded, leaving the three acceleration parameters from which discards were made in the order $\ddot{y}_s$, $\ddot{\phi}$ leaving $\ddot{y}_f$.

A regression run on the supersonically initiated manoeuvres (run 3 of Table 3) produced much the same results with ζ taking the place of $\ddot{y}_s$ in a four-parameter formula. The accuracy was slightly improved but this was to be expected because the sample covered a smaller range of air speed. Because of lack of subsonic data and because ζ was considered one of the more difficult parameters to measure, preference was given to the previous four-parameter formula.

The preference of the programme for $\ddot{\phi}$ suggested that the programme was in effect finding an adjustment to the lateral accelerations for the fact that the accelerometers were positioned well above the roll axis (see Fig.3), and were therefore picking up an acceleration component caused by $\ddot{\phi}$. Datum line values of $\ddot{y}_s$ and $\ddot{y}_f$ were calculated by applying adjustment terms produced by multiplying $\ddot{\phi}$ by the distances above the horizontal datum line of the sensitive axes of the accelerometers*. Applying the regression programme to this data resulted in $\ddot{\phi}$ being discarded much earlier, immediately after the yawing parameters (see run 2 of Table 3). There was evidence, though, that a small contribution from $\ddot{\phi}$ was still required.

4.3 Parametric formula selected for Lightning

The formula selected derives fin root bending moment from roll and acceleration measurements as follows:-

$$BM_{root} = 0.1640 \frac{\dot{\phi} q}{V_t} + 109.7\ddot{\phi} + 32300\ddot{y}_f + 31780\ddot{y}_s$$

where BM_{root} is in units of N m and the parameters in units of (deg/s) $\frac{N/m^2}{m/s}$, deg/s^2, g and g respectively.

The total correlation coefficient was 0.992 and the standard deviation of the error expressed as a percentage of the rms value of the actual fin root bending moment maxima and minima 12.6%. Parametrically derived values of fin root BM are shown plotted against strain derived values in Fig.5.

The relative importance of the contributions from each of the four parameters is indicated by their partial regression coefficients whose values, expressed as a percentage of their total, are:-

$\ddot{y}_f$ - 51.5%

$\ddot{y}_s$ - 24.5%

$\ddot{\phi}$ - 19.5%

$\dot{\phi}$ - 4.5%

$\ddot{y}_f$ is seen to be the major contributor; however, there is considerable variation in individual cases and the contribution from $\dot{\phi}$, the smallest contributor, can be significantly large. The contribution from $\ddot{\phi}$ arises largely from the need to adjust for the vertical offset of the lateral accelerometers above the

* It would have been preferable to refer acceleration positions to the roll inertia axis had its position been known.

fuselage horizontal datum line. Using adjusted values of lateral acceleration reduces the contribution of $\ddot{\phi}$ to 4.2%. Examples showing the time histories of the contributions from individual parameters together with a comparison of the parametrically and strain derived load time histories are given in Fig.6a to e. The last three of these examples refer to cases not included in the regression analysis.

4.4 Single parametric formula

Although accuracy is not to be discarded lightly, occasions arise when the requirement for simplicity is paramount and a loss of accuracy is acceptable in the interests of simplicity. Considerable simplification both in data collection and analysis results from the reduction of the parametric formula to a single parameter and this case is therefore discussed in some detail.

In the study of the Lightning, of the parameters measured directly, the most accurate single parameter for providing information on fin root bending moment loads was shown by the regression analysis to be angle of sideslip β adjusted according to the dynamic pressure q (see Table 4 for accuracy of single parametric formulae). This result, however, has to be treated with caution since both the airstream direction sensor and the vane, either of which could be used to sense angle of sideslip, were subject to serious malfunctions under certain flight conditions (see Appendix A) such that they could fail to indicate fin loads or produce false indications of large fin loads. Instances of severe malfunctions were not included in the regression analysis, although some milder instances may have been included unwittingly. While such malfunctions may have been peculiar to the Lightning installation, in general it is difficult to find positions for sideslip sensors which are free from significant shock wave and interference effects throughout a wide range of flight manoeuvres and Mach number. Mounting the sideslip sensor in front of the fin could help to surmount some of these difficulties but not all.

It may be preferable to use a parameter such as acceleration or rate of rotation, the sensors for which operate in an enclosed environment, i.e. within the aircraft. The regression analysis indicated that, of those measured directly on the Lightning, the best single parameter of this type was lateral acceleration at the fin. The accuracy of this parameter would have been better had the sensor been mounted lower down nearer the base of the fin as shown by the improvement in accuracy when $\ddot{y}_{f\mathfrak{L}}$ is used rather than $\ddot{y}_f$.

The optimum location for a single acceleration sensor can be obtained from the parametric formula containing the three accelerations $\ddot{\phi}$, $\ddot{y}_s$, $\ddot{y}_f$, on the assumption that the fuselage behaves as a rigid body. The position is found to be extremely close to the average position of the CG of the aircraft as flown in the flight trials (see Fig.3). As already stated it was impossible in the case of the Lightning to mount an accelerometer in the region of the CG but in general it may well be feasible to do so, in which case the findings of the Lightning study are that lateral acceleration can provide a better indication of fin root bending moment than any other single parameter. In practice, some compromise in location will probably be necessary and in considering alternatives, it should be borne in mind that mislocation along the normal axis can be expected to produce more serious errors than along the longitudinal axis. The reason for this lies in the greater magnitude of rolling compared with yawing acceleration experienced by swept wing aircraft, and in the fact that correlation between yawing and lateral acceleration (see Table 5) allows some correction to be made for the unwanted yawing component by modifying the coefficient of lateral acceleration, whereas the lack of correlation between rolling and lateral acceleration allows no such correction.

The fit of the parametric formula containing the single parameter $\ddot{y}_{opt}$ is shown in Fig.7. It is only slightly less accurate than that of the selected parametric formula (Fig.5).

It is important not to interpret parametric formulae in too simple a manner when drawing inferences as to the aircraft behaviour and loading actions associated with the fatigue loads, particularly when the number of parameters in the formula has been severely reduced. Because parameters are intercorrelated (see Table 5), one parameter can, to some extent, compensate for the discard of another if its coefficient in the parametric formula is suitably adjusted - a process evident in the regression analysis. Furthermore, when the correlation between the two parameters is high, the choice of parameter for inclusion in the formula is likely to be dictated by the relative amounts of noise present in the respective signals. Hence acceptance of a parametric formula at its face value as an indicator of the actual aircraft behaviour and loading actions associated with the fatigue loads can be misleading, and can result in mistaken lines of approach both in the field of load suppression and in attempting to derive coefficients for parametric formulae from aerodynamic derivatives.

4.5 The effect of Mach number on the acceleration-load relationship

In order to see whether the relationship between fin lateral acceleration and fin root bending moment was subject to significant Mach number effects, the regression programme was run with the subsonic and supersonically-initiated manoeuvres treated separately. The supersonic coefficient for $\ddot{y}_{f\mathcal{L}}$ was found to be some 15% greater than the subsonic, a result in accordance with an outboard shift of c_p in the supersonic cases. The actual Mach number effects may have been larger because the aircraft inertia tended to be lower for the supersonic manoeuvres (considerable fuel was consumed in getting clear of land and attaining supersonic speed) and this could be expected to produce a decrease in the coefficient of $\ddot{y}_{f\mathcal{L}}$ counteracting to some extent the increase associated directly with Mach number. It is questionable whether inaccuracies indicated by this variation merit correction by conditioning acceleration according to Mach number (parameters other than acceleration may also require conditioning but these have not been investigated). Provided a realistic proportion of supersonic to subsonic cases are included in the sample on which the parametric formula is based, an acceptable accuracy is probably attainable without this conditioning, having regard to the general scatter and the tendency of negative and positive errors to cancel each other out when data is expressed in terms of counts of load occurrences. Alternatively different parametric formulae might be used for subsonic and supersonic cases, necessitating only a crude indication of the occurrence of supersonic flight when collecting operational data.

5 ACCURACY

It is not proposed to discuss the accuracy of the parametric method developed for the Lightning fin in detail but rather make a few general points in the light of experience with the Lightning.

In assessing the degree of accuracy required for an operational method of measuring fin fatigue loads, it is worthwhile bearing in mind the current shortage of operational data on such loads and the somewhat crude practice of predicting fin fatigue load spectra by applying a factor of 3 to the predicted occurrences of gust loads to allow for all other loading cases including manoeuvres. Clearly it is unnecessary to attain a high degree of accuracy in order to improve this situation. Furthermore there is a strong case in the field of operational measurement for favouring simplicity even at the expense

of potential accuracy. In fact, the simpler method may well, in the long run, prove the more accurate due to its greater reliability and easier detection of faults.

The parametric method has an advantage in that it provides some guidance as to the possible loss of accuracy associated with simplification. Simplification in the parametric method can readily be effected by reducing the number of parameters with, in general as the number gets small, a reduction in accuracy as indicated by the fit of the parametric formula to the sample loads. For example, in the case of the Lightning fin root bending moment, reducing the number of parameters from four to one reduces the total correlation coefficient from 0.992 to 0.954*. However, too much emphasis should not be placed on such statistical accuracy since not only does its wider applicability depend on the validity with which the sample chosen for the regression analysis represents the total future population of loading cases, but also it is by no means the only consideration affecting overall accuracy. An important item to take into consideration is the behaviour of the parametric combination between matched points.

A more valid assessment of accuracy is obtainable by comparing the total time histories of the parametrically and strain derived loads and, in particular, the load distributions arising from them. Because of limitations in the data processing facilities at the time of analysis, this comparison could not be made for the bulk of the Lightning data without excessive labour, and comparison was limited to a few cases. These relate both to the data on which the parametric combination is based (time histories compared in Fig.6a, b and c) and to data not included in the regression sample (time histories compared in Fig.6d, e and f). The comparison should have been especially interesting in the case of flight refuelling (Fig.6d) since this was a type of loading case not included in the sample. Unfortunately, the loads proved much smaller than expected so that this comparison is not as conclusive as hoped. The poorest fit in time histories is that for the supersonic manoeuvre (Fig.6c). The fit can be improved by using the parametric formula in which $\ddot{y}_s$, lateral acceleration at the spine, is replaced by ζ, rudder angle factored by dynamic pressure (Fig.8). The contribution from ζ is small and the improvement is probably associated more with a reduction of acceleration errors peculiar to the Lightning than with the intrinsic value of ζ as a general parameter for representing fin root bending moment.

* The significance of these accuracies and their relation to the standard deviation of the error can best be appreciated from a study of Fig.9 which shows the fit of matched points for a series of parametric formulae as parameters are successively discarded.

A comparison of the load levels exceeded taken from the combined time histories of Fig.6 is shown in Fig.10. The tendency for negative and positive errors to cancel out has resulted in some improvement but the amount of data is too small for this tendency to be effective except at the smaller load levels. Errors tend to be slightly on the conservative side due to the parametric peaks and troughs not always coinciding in time with those of the strain derived loads so that their values may be outside those used in matching. This conservatism can provide some compensation for small dynamic loads unrepresented in the parametric formula because of the filtering. An example where such compensation is applicable is shown in Fig.11 where the unfiltered root bending moment measured by means of strain gauges compares favourably with the parametrically derived bending moments.

6 CONCLUSIONS

Based on a study of flight measurements on a Lightning Mk.T5, a method has been developed for producing, from sample time histories and loads measured in manoeuvres and other loading cases, a combination of parameters other than strain to provide operational information on overall fin root loads. The method consists of optimising the matching of the parametric combination to the required load at the instants when the latter attains maximum and minimum values of significance in fatigue. It is then necessary to check that the parametric combination does not produce spurious maxima and minima between matched points. The method requires the frequency band to be confined to rigid body frequencies; small dynamic effects due to structural oscillations are covered by the tendency of the parametric combination to overestimate slightly the rigid body loads because of the behaviour between matched points. Larger dynamic effects may need to be covered by the introduction at a later stage of dynamic factors appropriate to the particular locality. To provide information on these dynamic factors, the parametric method may need to be supplemented by information from strain counters or fatigue sensors.

The study has been concentrated on fin root bending moment, but the method is equally applicable to fin root shear and torque.

The most practical parametric combination to provide information on the Lightning fin root bending moment consists of lateral acceleration at the fin and at the spine, roll rate, conditioned by multiplying it by dynamic pressure and inverse true airspeed and roll acceleration - the function of the latter is mainly to adjust for offset of the lateral accelerometers above the roll axis.

Had it been physically possible to mount a lateral accelerometer at the optimum position near the aircraft CG, the number of parameters could have been reduced to two, namely roll rate conditioned as above and lateral CG acceleration, with no loss of accuracy. Omission of the roll rate term would have resulted in a slight loss of accuracy (total correlation coefficient reduced from 0.992 to 0.990).

Under operational circumstances demanding the utmost simplicity, the Lightning study indicates that the most practical single parameter for obtaining information on overall fin root bending moment is lateral acceleration measured near the CG. Angle of sideslip, scaled according to dynamic pressure, showed potential for use as a single parameter but the reliability of measurement would need to be improved.

Consideration should be given to using a parametric combination with different coefficients for subsonic and supersonic cases. The Lightning study indicated an increase of 15% in the coefficient relating fin lateral acceleration to fin root bending moment for supersonic cases as compared with subsonic cases.

Effects due to changes of mass associated with carriage of stores and fuel usage (all up weight varied by less than ±9%) were not detectable within the general scatter.

Although high correlations have been obtained between parametric combinations and the required load at matched points, overall accuracy depends also on the behaviour of the combination between matched points. Limitations in the data processing facilities at the time of analysis make this accuracy unduly laborious to assess fully. Indications are that, in terms of some form of distributional count, the parametric method can, without undue complication, produce results of acceptable accuracy.

Appendix A

INSTRUMENTATION AND FLIGHT TRIALS

Flight instrumentation

Lightning aircraft XM 967, a Mk.5 prototype, arrived at RAE Farnborough with a large amount of instrumentation already installed having previously been engaged on flight trials by BAC at Warton. These trials in which fin loads were measured, mainly during rolling manoeuvres, were made to investigate the reason for the loss of a Lightning aircraft when carrying out similar manoeuvres.

Three recorders had been installed on the aircraft, an A1322 recorder, a CID recorder (both producing photographic trace records) and an Ampex AR 200 magnetic tape recorder. The trace recorders were used for monitoring handling parameters and the tape recorder monitored the remaining handling data and signals from strain gauges installed in the fin.

During the trials at Warton the method used to record the signals from the fin strain gauges was to record the output from 24 bridges on each of two tape channels by multiplexing, each bridge being sampled 16 times per second. The ground equipment for demultiplexing the information on the flight tapes had been designed by BAC and was a permanent installation in their Warton data reduction centre. It was also used in the analysis of records from other flight trials carried out by the Firm and was not available for the replay and analysis of RAE flight tapes. It was therefore decided, before the trials at RAE commenced, to bypass the multiplexing switch and to record the output from eight selected bridges continuously (the number of channels available for strain gauges being limited by the number of data amplifiers used in the previous system). Although gauges were attached at a large number of positions over the fin, for the purpose of the RAE trial it was decided that measurements could be confined to those gauges attached across a section near the root of the fin. Eight of the available ten strain gauge bridges were selected after analysing the results from an applied load calibration of the fin made by BAC in 1969, in which loads were applied singly at 60 pads, 30 each side of the fin. A repeat load calibration, done in early 1971, confirmed the earlier selection. These gauges were used throughout the trial.

The remaining six channels on the tape recorder were used to record a time base and a selection of five parameters. Variations in the parameters recorded were made during the trial; it was also possible, if required, to

record more than five parameters but only at the expense of strain gauge channels.

A list of parameters available for recording on the three recorders is given in Table 1 and the location of the major items of equipment are shown in Fig.1. The positions of the strain gauge bridges near the root of the fin and of the accelerometers are shown in Figs.2 and 3.

Aircraft serviceability

Although the aircraft was engaged on the fin load measurement trials for a considerable time (approximately 4 years), due to long periods of aircraft unserviceability and other reasons, e.g. experimental instrumentation unserviceability, unsuitable weather for the trial and a shortage of pilots on occasions, it was available for experimental flying for less than one quarter of this time. Due to the intermittency of the flying there was a considerable turn-over of pilots resulting in a higher proportion of crew training flights than would otherwise have been necessary. The extended time scale and frequent dismantling of parts of the aircraft for servicing purposes also produced problems with the experimental instrumentation which was a further factor in reducing the number of useful experimental flying hours. Nevertheless, over 100 experimental flights were made during the trial although these were effectively reduced due to the necessity to repeat a number of the flight cases because of the limited number of recording channels available.

Flying programme

The flying programme commenced with the aircraft carrying out a series of simple manoeuvres based on design cases for the fin. These were steady sideslips and the rapid application followed by the sudden release of the rudder (rudder kicks). These manoeuvres were done at three nominal heights of 2000ft (609.6m), 20000ft (6096m) and 40000ft (12192m) and at three indicated airspeeds at each height, 200, 400 and 550kn. They were performed with the aircraft clean and also carrying one or two Firestreak missiles on the Blue Jay pack attached to the underside of the fuselage (see Fig.1). A further variation was that the manoeuvres were performed with the rudder stabilisation system switched on and off although the former of these cases was not completely covered owing to unserviceability of the stabilisation system which necessitated flying the aircraft for a long period with the rudder stabilisation system rendered inoperative.

Later in the trials, operational type manoeuvres were performed by ex-Squadron pilots; these consisted of breakaway manoeuvres, rolling pullouts and aerobatics which included aileron rolls. Again these manoeuvres were done with the aircraft clean and also carrying Firestreak missiles. Measurements were also taken when the aircraft flew in turbulence at low altitudes at indicated airspeeds of up to 550kn and when the aircraft carried out a simulated flight refuelling operation. For this latter case a standard refuelling probe was fitted to the aircraft and a number of dry refuelling engagements were made behind a Victor tanker aircraft.

During the trials the all-up-weight of the aircraft varied from a maximum of approximately 15875kg when two Firestreak missiles were carried and with a full fuel load, down to a minimum weight of 12700kg with the aircraft clean and minimum safe fuel load, a variation of ±11% about the mean weight. The weight variation during the period of the flight when measurements were taken would, however, have been at least 2% less than this. Weight during supersonic manoeuvres, because of fuel consumption in reaching the south coast and attaining supersonic speed (supersonic flight was allowed only over the sea) was less on average than that for subsonic manoeuvres, the difference being of the order of 5%. The Firestreaks weighed 141.4kg each and could be expected to increase the total yawing moment of inertia of the Lightning by about 0.6%.

Sideslip measurements

The aircraft arrived at RAE having two independent systems for measuring sideslip angle installed. One system used an airstream direction sensor, the other system used a Penny and Giles windvane.

Due to an unfortunate choice of position for the airstream direction sensor the sensitivity of this system varied widely with Mach number, the variation being particularly rapid in the transonic region (see Fig.13); this complicated the computation but was otherwise acceptable. Malfunctions, also attributed to the positioning of the sensors occurred from time to time in both systems under certain flight conditions. These are discussed below.

Airstream direction sensor

This system consisted of a sensor mounted in the airstream from which differential pressure was fed to each side of a paddle. The paddle rotated until the pressure each side was equalised and its position was monitored by means of a rotary potentiometer. The sensor was installed on the top of the

fuselage, on the centre line, between the jet intake lip and the windscreen. This type of installation had been the subject of an EEA Ltd. Flight Test Note[8]. Due to the instrument's rapid response characteristics it was considered particularly suitable for use in dynamic manoeuvres.

In the Lightning trials, under certain conditions of flight, the system became unduly sensitive and in some cases severe hash on the record rendered the results unusable. Similar hash had been observed in the firm's tests[8] and was attributed to unsteady airflow associated with engine intake spillage, and to conditions of high incidence in subsonic flight. An alternative mounting position for the sensor, possibly on the underside of the fuselage on the centre line might have reduced some of the effects caused by unsteady flow mainly in the high incidence case but mounting a sensor in this position on a Lightning was not considered to be mechanically possible and could have produced similar hash at negative incidence.

Penny and Giles windvane

The vane detecting the direction of the airflow was mounted on the pitot boom which projected from the underside of the engine intake on the aircraft centre line. The vane was attached at a position approximately 1m ahead of the intake lip. This system had a more stable response during manoeuvres than did the ADD system but in certain flight conditions, particularly when flying at high angles of incidence subsonically the system response was considerably reduced. At times there were indications that the vane had been affected by water or ice as the waveform of the output signal became distorted and the peaks were clipped.

Examples of errors in the sideslip measuring systems

Fig.14a, b and c illustrates some of the errors which occurred with the two systems of measuring sideslip. The figures show traces from the airstream direction sensor and the windvane. A trace has also been included from a strain gauge bridge responsive to bending moment on fin spar 3. The sideslip traces have not been adjusted for variations in dynamic pressure, which affect their relation to fin load, but values of Mach number and altitude have been added to the figures.

Fig.14a illustrates the behaviour of the airstream direction sensor during a descent from altitude. The signal from the sensor shows periods of high sensitivity, and high frequency hash is also present due to unsteady air flow probably due to air spillage from the engine intake. The trace from the sideslip vane, being situated ahead of the intake, has not been affected.

In Fig.14b, the airstream direction sensor, due to its position on the aircraft, is again showing periods of over-sensitivity and high frequency hash is again present. In the latter part of the sample, when the aircraft was in reasonably level high subsonic flight, the vane has also been affected, the output falling to a very low level.

Fig.14c, is a record of a supersonic manoeuvre and recovery. In this example only the airstream direction sensor was being used to record sideslip angle. It can be seen that the sensor, due to its installation deficiencies has failed to respond sensibly to the first half of the manoeuvre but during the second half it has behaved normally. During the recovery period the signal has become very large and the high frequency hash associated with unsteady airflow is again present.

Appendix B

LOAD DISTRIBUTION IN THE LIGHTNING FIN

Additional information on the overall fin loads, spanwise load centre, and distribution of local load at the fin root (rib 1) is presented in Table 4 and Fig.12. The information has had to be extracted from flights other than those used to derive the parametric formulae since it was not possible to record simultaneously on the main recorder all the eight strain signals as well as the full number of parameters required for the load distribution and the parametric study respectively. The information is presented as being of intrinsic value in itself, and because it exemplifies the type of additional information available from special flight tests, the primary objective of which is the setting up of a parametric formula. At a later stage, such additional information may prove useful in interpreting operational results from the parametric formula in terms of local loads.

The overall fin root bending moment and shear loads are derived from strain measurements using the regression formulae 1 and 2 of section 4.1. The spanwise centre of load (combined aerodynamic and inertia loads) is obtained from the ratio of overall bending moment to shear load and is given as a distance outboard of, and normal to, rib 1. In discussing local loads in individual spars, the average of the tensile and compressive boom strain is taken as an indicator of the local bending moment in the spar. Similarly the average web shear strain is taken as an indicator of the local shear load in the spar.

The centre of load shows considerable movement varying from 0.93 to 1.57m (36.5 to 62in), the most inboard positioning of the load centre tending to occur during steady sideslips when the loading is purely aerodynamic (see Table 6). As the centre of load moves inboard, spar 2, the second spar back from the leading edge, tends to carry a slightly greater proportion of the total bending moment whereas the proportion carried by spar 4, one of the mid spars, is more constant (Fig.12). An analysis of shear in spar 2 and in the rear shear wall shows that the proportion of shear load in spar 2 to total shear load varies little with spanwise load centre, whereas that in the rear shear wall tends to decrease rapidly even opposing the main shear load as the load centre moves outboard (Fig.12). Scatter from the main trend occurs mostly in rolling manoeuvres such as aileron and barrel rolls.

No attempt is made to explain these results since the effects are obviously complex with angle of sweep, rudder loading and relative magnitude of aerodynamic

to inertia loading all contributing to the effects observed. Further detailed analysis of the measurements would be advisable for a clearer understanding. The limited results obtained do, however, go some way towards demonstrating that the proportion of total load taken by individual spars does not vary widely with the exception of shear load in the rear spar. Thus for spars 2 and 4 the indications are that parametric formulae for total bending moment and shear load could readily be interpreted in terms of local root loads.

Table 1

DETAILS OF MANOEUVRES AND LOADING CASES USED IN DERIVING PARAMETRIC COMBINATION

Flight and run No.	
121-1	Rolling pullout. 300kn, 14000ft, 2g left. Autostabilisers on.
-2	Rolling pullout. 300kn, 14000ft, 2g right. 350kn, 2.5g left. Autostabilisers on.
-3	Rolling pullout. 350kn, 14000ft, 2.5g right. Autostabilisers on.
-4	Rolling pullout. 400kn, 14000ft, 3.5g left, right. Autostabilisers on.
123-1	Aileron rolls. 300kn, 30000ft. Left, autostabilisers on; left, autostabilisers off; right, autostabilisers on; right, autostabilisers off.
137-1	Series of yawing manoeuvres, roll suppressed. 220kn, 20000ft. Autostabilisers on.
-2	As 137-1, 350kn.
-3	Aileron rolls, minimum yawing. 350kn, 20000ft. 2 left, 1 right. Autostabilisers on.
124-1	Sideslips. 200kn, 4000ft. 10° port, 10° starboard applied. Autostabilisers off.
-2	Sideslips. 200kn, 4000ft. 10° port, 10° starboard applied. Autostabilisers on.
-3	Sideslips. 400kn, 4000ft. 6° port, 6° starboard applied. Autostabilisers on.
-3A	Sideslips. 550kn, 4000ft. 2° port, 2° starboard applied. Autostabilisers on.
-4	Sideslips. 200kn, 20000ft. 10° port, 10° starboard applied. Autostabilisers on.
-5	Sideslips. 410kn, 20000ft. 6° port, 6° starboard applied. Autostabilisers on.
135-1	Moderate turbulence. 350kn, 1500ft. Autostabilisers on.
136-1	Moderate turbulence. 400kn, 2000ft. Autostabilisers on.
123-2	Aileron rolls. 360kn, 30000ft. Left, autostabilisers on; left, autostabilisers off; right, autostabilisers on; right, autostabilisers off.
153-2	Missile breakaway manoeuvre. 590kn, 24000ft initially. 40° starboard turn, 3g; pull up at 4g; invert, pull through 3g; recover. Autostabilisers on.
151-2	Roll left. 550kn. 20000ft. Autostabilisers on.
-3	Roll right, 550kn. 20000ft. Autostabilisers on.
-4	Roll left, roll right. 550kn. 20000ft. Autostabilisers off.
154-1	Missile breakaway manoeuvre. 520kn, 25000ft initially. Hard turn through 90° to port; pull up to 33000ft; invert, pull, recover. Autostabilisers on.
152-1	Rudder kicks. 550kn, 20000ft. Starboard, port, autostabilisers on; starboard, port, autostabilisers off.

The rudder autostabiliser was not functioning on the above flights, except for 151, 152, 153 and 154. The aileron and elevator autostabilisers were functioning on all the above flights.

No missiles were carried on the above flights.

Table 2

LOAD PEAKS AND TROUGHS AND SIMULTANEOUS VALUES OF PARAMETERS

Flight and run number	BM_{root} N m	$\dot{\phi}$ deg/s	β_p deg	$\dot{\psi}$ deg/s	$\ddot{\phi}$ deg/s^2	$\ddot{\psi}$ deg/s^2	$\ddot{y}_F$ g	$\ddot{y}_S$ g	ζ deg	V_T m/s	q kN/m^2	M
121-1	3294	27.105	2.789	-1.761	5.773	-2.094	0.07399	0.01624		193.07	16.241	0.5964
	-3425	130.230	-1.373	-0.055	3.444	3.341	-0.07569	-0.03942				
121-2	-5935	-24.716	-3.251	0.854	6.232	6.786	-0.15707	-0.00594		193.07	16.241	0.5964
	6496	50.162	1.419	-4.619	2.624	-3.497	0.12914	0.01274		224.20	22.557	0.6925
121-3	4195	23.506	0.688	-2.362	-17.384	-2.079	0.12342	0.04072		224.20	22.557	0.6925
	-7933	-25.529	-1.869	1.664	-12.136	8.464	-0.12688	-0.03342				
	4611	2.202	0.783	2.562	5.412	-5.643	0.11877	0.01700				
121-4	7393	46.319	1.335	-3.876	-4.920	-2.524	0.19059	0.04224		254.96	30.146	0.7875
	-6423	-19.129	-1.785	0.794	-8.200	7.187	-0.11012	-0.00864				
123-1	10976	-16.054	4.838	2.561	46.904	-20.099	0.22317	-0.03240		245.17	16.170	0.8081
	11373	-22.968	3.578	3.296	-10.988	-20.545	0.39847	0.03060				
	-15918	10.351	-5.068	-2.635	-4.264	28.683	-0.42507	-0.07020				
	-16378	153.980	-4.123	-2.577	-9.512	28.750	-0.44794	-0.03580				
137-1	-13413	6.282	-6.945	0.343	-26.896	14.924	-0.25922	-0.11180		155.83	8.436	0.4928
	-10619	-0.524	-7.102	0.668	9.184	8.316	-0.25283	-0.13240				
	-12903	13.992	-6.981	-0.862	12.628	17.152	-0.31827	-0.08580				
	15289	-13.944	6.703	0.838	-4.756	-18.934	0.43518	0.15020				
	-13807	13.373	-8.313	0.164	6.068	14.330	-0.34394	-0.16660				
	14437	-17.657	6.134	1.217	-8.200	-21.087	0.42241	0.10320				
	14711	-10.565	0.176	-0.892	4.756	-20.864	0.39514	0.09380				
137-2	-20942	-2.762	-4.886	-0.408	-7.052	11.212	-0.36203	-0.26100		244.26	22.559	0.7724
	21365	1.869	4.178	0.861	0.656	-16.186	0.43265	0.21680				
	23548	0.586	4.904	0.691	-12.300	-17.523	0.52721	0.29420				
	-21670	- 0.921	5.607	0.364	2.296	11.806	-0.32678	-0.31780				
	13688	-1.450	3.542	0.727	11.972	-7.202	0.27292	0.14440				
	-17256	10.851	-4.202	-0.765	35.096	19.528	-0.49010	-0.17120				
137-3	- 7133	-27.560	-1.762	1.743	13.448	4.455	-0.15042	-0.09176		244.26	22.559	0.7724
	6607	-8.508	2.155	0.856	38.048	-6.757	0.07169	+0.01292				
	- 5128	68.315	-1.049	0.962	2.296	7.128	-0.14989	-0.08946				

Table 2 (continued)

Flight and run number	β^M_{root} N m	$\dot{\phi}$ deg/s	β_p deg	$\dot{\psi}$ deg/s	$\ddot{\phi}$ deg/s^2	$\ddot{\psi}$ deg/s^2	$\ddot{y}_f$ g	$\ddot{y}_s$ g	ζ deg	V_T m/s	q kN/m^2	M
124-1	-7860	1.878	-4.414	0.567	15.416	5.428	-0.21320	-0.11766		110.35	6.813	0.3286
	8875	0.042	5.134	1.746	-1.640	-2.487	0.14297	0.11388				
124-2	-8283	2.838	-5.395	-1.307	2.936	2.599	-0.13207	-0.10044		110.35	6.813	0.3286
	10070	-1.836	5.298	-1.107	-9.512	-7.499	0.21586	0.12124				
124-3	-16317	-1.310	-2.748	0.394	3.608	5.717	-0.27651	-0.20520		223.09	30.262	0.6647
	23384	-6.552	3.830	-0.966	-24.764	-13.513	0.50460	0.31420				
124-3A	-16524	-1.478	-0.978	-0.938	-2.460	1.262	-0.19471	-0.22700		306.53	62.526	0.9129
	6593	-0.632	0.096	-0.344	11.152	-9.073	0.12741	0.02340				
	13692	0.265	0.692	-0.276	-0.820	-1.819	0.15215	0.13280				
	-5846	6.328	-0.176	-0.276	-20.664	6.430	-0.10254	-0.02720				
124-4	-8889	18.224	-5.377	1.612	16.236	9.794	-0.25802	-0.08206		142.25	6.957	0.4498
	4512	-11.166	2.125	1.195	18.860	-6.549	0.08791	-0.02186				
	8337	-2.950	4.456	-1.366	-16.400	-9.348	0.22982	0.12732				
	-3270	13.221	-1.683	-2.420	30.832	5.190	-0.10507	0.00718				
124-5	-18266	4.572	-3.153	0.183	11.480	7.128	-0.34327	-0.26320		283.99	32.003	0.8980
	9673	-3.612	0.950	-0.670	23.944	-17.820	0.23381	-0.01440				
	18383	-4.892	2.658	-0.414	-18.532	-10.321	0.34966	0.20120				
	-13195	9.350	-1.493	-0.819	-0.164	21.681	-0.36655	-0.07020				
135-1	7064	-7.653	1.233	-0.932	-6.396	-7.878	0.18075	0.02884		194.40	24.082	0.5738
	-5952	10.714	-0.828	-0.314	2.296	8.516	-0.13938	-0.04596				
	-6834	11.441	-1.334	0.092	4.592	7.841	-0.17942	-0.05430				
	5921	-5.698	0.973	-0.708	7.872	-7.856	0.12967	0.01402				
	-8903	4.845	-1.606	0.414	-10.660	9.719	-0.17356	-0.06112				
	-6149	10.029	-1.236	0.713	4.756	7.299	-0.15893	-0.08100				
	-6423	5.600	-1.134	1.087	-4.920	8.130	-0.14377	-0.02468				
	10884	-11.084	1.766	-0.281	-6.724	-13.068	0.27544	0.10436				
	-9008	10.034	-1.595	0.045	7.052	13.751	-0.24658	-0.04390				
136-1	7222	-3.978	1.045	-1.172	-6.888	-7.574	0.16000	0.06450		217.63	30.357	0.6436
	6013	-2.674	0.793	-0.150	7.216	-7.239	0.13180	0.01732				
123-2	3712	-66.870	-0.441	3.264	-27.880	0.386	-0.01609	0.03120		293.51	24.719	0.9674
	3658	-16.916	0.324	0.367	69.700	-6.088	-0.06091	-0.07680				
	-5729	-102.230	-0.851	5.354	-16.072	2.005	-0.07049	-0.07540				
	3867	-4.283	0.374	0.245	95.940	-5.643	-0.10121	-0.10700				
	-776	-35.790	-1.078	-0.713	-81.180	14.553	-0.06956	0.11580				
	7339	-12.083	1.294	0.830	14.104	-11.657	0.15774	0.04360				
	3670	85.193	0.227	-3.588	23.944	-3.416	-0.03338	-0.10660				
	-4296	16.794	-0.564	-0.656	-27.552	+6.756	-0.04442	0.04480				

Table 2 (concluded)

Flight and run number	BM_{root} N m	$\dot{\phi}$ deg/s	β_p deg	$\dot{\psi}$ deg/s	$\ddot{\phi}$ deg/s^2	$\ddot{\psi}$ deg/s^2	$\ddot{y}_F$ g	$\ddot{y}_S$ g	ζ deg	V_T m/s	q kN/m^2	M
153-2	5083	41.929	-0.473	0.307	3.874	-2.242	0.04279	0.03280	-1.080	405.37	70.838	1.3010
	-7588	-32.635	-1.092	-0.703	-10.074	3.495	-0.14005	-0.08480	0.659	387.29	61.851	1.2448
	-4848	93.614	-0.047	0.903	-39.524	1.808	0.22809	-0.01960	-0.506	321.80	31.643	1.0588
	7346	9.701	1.285	0.295	-9.299	-5.242	0.20628	0.07280	1.073	312.37	28.122	1.0334
	-12718	-79.370	-2.054	4.445	3.870	6.313	-0.24685	-0.12320	-1.469	292.99	23.681	0.9704
	4996	5.266	1.042	0.088	24.026	-2.434	0.04545	0.02220	3.185	301.83	27.320	0.9910
151-2	-4022	-73.778	-0.336	-0.865	-12.087	0.272	-0.03362	-0.04340	0.369	361.36	58.447	1.1427
	-9422	-29.833	-0.797	-1.090	77.818	0.665	-0.33330	-0.17080	-2.648			
151-3	4564	48.979	0.312	-0.161	-5.428	-0.838	0.03546	0.02744	-0.002			
	3928	25.740	0.332	0.772	-31.767	-1.970	0.14138	0.07778	1.583			
151-4	-8269	-68.968	-0.799	1.082	-5.346	0.757	-0.10786	-0.09020	0.024			
	-7572	-67.184	-0.635	-1.266	45.182	1.767	-0.21280	-0.12700	0.032			
	3343	56.656	0.292	0.181	4.412	-0.101	0.01298	-0.01640	-0.032			
	2822	37.590	0.152	1.682	-41.541	-2.273	0.12068	0.04600	-0.031			
154-1	-8433	-48.974	-1.227	0.867	37.982	2.949	-0.20562	-0.14920	-1.156	369.16	52.764	1.1911
	9743	48.988	0.923	-2.024	56.580	-6.010	0.05710	-0.03580	0.582	307.94	35.272	0.9855
	-4639	-1.316	-0.579	-1.269	-19.368	7.787	-0.06542	0.01080	-0.360	305.87	34.725	0.9787
	-9250	-114.470	-1.108	3.632	-32.554	7.121	-0.12985	-0.03160	0.608	270.57	21.417	0.8862
	6921	7.816	1.329	1.013	-13.169	-5.767	0.17755	0.06500	0.593	264.18	19.594	0.8689
	-10006	-45.720	-3.080	4.178	-27.126	6.080	-0.14816	-0.05420	-2.004	255.77	17.266	0.8464
	6355	-2.798	1.564	0.401	-0.771	-3.878	0.14976	0.06940	1.533	265.85	19.584	0.8761
152-1	-6982	9.174	-0.642	-0.085	14.022	3.686	-0.14803	-0.09820	-3.923	361.36	58.447	1.1427
	3026	-2.485	0.175	0.162	-14.416	-3.666	0.11386	0.04740	-0.158			
	10187	-12.424	0.784	0.086	-18.991	-5.474	0.23355	0.14240	4.858			
	-3390	2.437	-0.344	-0.085	19.221	4.696	-0.13885	-0.04280	0.102			
	-8945	10.146	-0.810	-0.239	28.438	6.706	-0.22517	-0.11960	-5.107			
	5970	-2.787	0.495	0.237	-39.983	-8.444	0.24618	0.08680	0.381			
	11098	-13.252	0.999	-0.137	-38.753	-8.888	0.32266	0.15760	4.747			
	8468	4.380	-0.765	-0.260	49.446	11.332	-0.32931	-0.13080	-0.528			

Table 3

ORDER OF ELIMINATION OF PARAMETERS AND ACCURACY OF MULTI-PARAMETRIC FORMULAE

Parameters in order of elimination	Total correlation coefficient and RMS error (% of RMS of BM_{root}) for formulae arising from successive eliminations	Remarks
Regression run		
1 $\ddot{\psi}\ \dot{\psi}\ \beta\ \boxed{\dot{\phi}\ \ddot{y}_s\ \ddot{\phi}\ \ddot{y}_f}$	0.993 0.993 0.993 **0.992** 0.990 0.975 0.954 12.1 12.0 11.9 **12.6** 14.1 22.6 30.3	Sub- and supersonic cases
2 $\ddot{\psi}\ \dot{\psi}\ \ddot{\phi}\ \beta\ \dot{\phi}\ \ddot{y}_{s\mathcal{C}_L}\ \ddot{y}_{f\mathcal{C}_L}$	0.993 0.993 0.993 0.993 0.991 0.990 0.971 12.1 12.0 11.9 12.4 13.3 14.6 24.0	As above but lateral accelerations adjusted for roll
3 $\ddot{\psi}\ \beta\ \ddot{y}_s\ \dot{\psi}\ \boxed{\zeta\ \dot{\phi}\ \ddot{\phi}\ \ddot{y}_f}$	0.996 0.996 0.996 0.996 **0.996** 0.990 0.978 0.910 10.7 10.5 10.2 10.2 **10.25** 12.7 24.6 42.1	Supersonic cases only - includes rudder angle
4 $\ddot{\psi}\ \beta\ \ddot{y}_{s\mathcal{C}_L}\ \dot{\psi}\ \ddot{\phi}\ \zeta\ \dot{\phi}\ \ddot{y}_{f\mathcal{C}_L}$	0.996 0.996 0.996 0.996 0.996 0.993 0.985 9.974 10.7 10.5 10.2 10.2 10.25 12.3 18.1 23.0	As above but lateral accelerations adjusted for roll
5 $\ddot{\phi}\ \dot{\psi}\ \dot{\phi}\ \dot{\psi}\ \beta$	0.973 0.973 0.973 0.970 0.956 23.6 23.4 23.5 24.5 29.5	Lateral transverse accelerations omitted.

Boxed formulae:- Selected formula $BM_{root} = 0.1640\dot{\phi}\frac{q}{V_t} + 109.7\ddot{\phi} + 32300\ddot{y}_f + 31780\ddot{y}_s$

Formula with ζ $BM_{root} = 0.2934\dot{\phi}\frac{q}{V_t} + 87.24\ddot{\phi} + 40280\ddot{y}_f + 0.009501\zeta q$

Table 4

ACCURACY OF SINGLE PARAMETRIC FORMULAE

Parameter	Standard deviation of error % of rms of BM_{root}	Correlation coefficient	Remarks
$\ddot{y}_{opt}$	14.1	0.990	Lateral acceleration (derived) at optimum location (see Fig.4)
$\ddot{y}_{f\mathcal{C}_L}$	24.0	0.971	Fin lateral acceleration adjusted for roll acceleration due to vertical offset
βq	29.5	0.956	Angle of sideslip factored by dynamic pressure
$\ddot{y}_f$	30.2	0.954	Fin lateral acceleration unadjusted
$\ddot{\psi}$	49.0	0.873	Yawing acceleration

Table 5

CORRELATION COEFFICIENTS RELATING INDIVIDUAL PARAMETERS TO EACH OTHER AND TO FIN BM_{root}

	β	$\dot{\phi}$	$\ddot{\phi}$	$\dot{\psi}$	$\ddot{\psi}$	$\ddot{y}_s$	$\ddot{y}_f$	$\ddot{y}_{s\mathcal{C}_L}$	$\ddot{y}_{f\mathcal{C}_L}$	ζ	BM_{root}
β	1	0.104	-0.102	-0.058	-0.812	0.859	0.918	0.902	0.920	0.592	0.956
$\dot{\phi}$		1	0.054	-0.333	0.080	0.080	0.024	0.106	0.041	-0.094	0.124
$\ddot{\phi}$			1	-0.166	-0.052	-0.412	-0.259	0.100	0.032	-0.382	-0.053
$\dot{\psi}$				1	-0.046	-0.018	0.004	-0.078	-0.046	-0.020	-0.076
$\ddot{\psi}$					1	-0.600	-0.904	-0.674	-0.951	-0.503	-0.873
$\ddot{y}_s$						1	0.855	-	-	0.632	0.860
$\ddot{y}_f$							1	-	-	0.599	0.954
$\ddot{y}_{s\mathcal{C}_L}$								1	0.843	0.578	0.921
$\ddot{y}_{f\mathcal{C}_L}$									1	0.530	0.971
ζ										1	0.560
BM_{root}											1

Table 6

OVERALL LOADS, SPANWISE LOAD CENTRE AND LOCAL STRAINS MEASURED AT FIN ROOT (RIB 1)

Flight and run number	Overall loads		Spanwise load centre	Local strains				Case
				Longitudinal*		Shear		
	BM	Shear		Spar 2	Spar 4	Spar 2	Rear wall	
	N m	N	m	μ strain	μ strain	μ strain	μ strain	
53.1	-2590	-1960	1.31	-49.9	-43.5	-45.6	9.1	Aileron rolls - roll and yaw auto-stabilisers on. 350kn, 10000ft.
	1700	1510	1.12	33.8	28.1	32.5	-2.0	
	3770	2940	1.28	62.5	63.9	75.8	-3.3	
	-2210	-1760	1.25	-44.2	-38.0	-42.2	6.5	
53.2	-3440	-2490	1.38	-58.3	-66.6	-50.2	9.8	
	2090	1970	1.06	36.5	36.1	48.3	34.4	
	4510	3090	1.46	66.0	77.6	61.4	-15.6	
53.3	-1990	-1390	1.43	-30.9	-34.2	-26.0	-17.5	Barrel rolls - roll and yaw auto-stabilisers on. 350kn, 10000ft
	1000	1070	0.93	17.5	18.0	18.5	7.1	
53.4	2990	2270	1.32	51.2	55.3	45.2	-11.7	
53.5	2470	1710	1.44	38.0	42.2	35.8	-20.2	Barrel rolls - roll and yaw auto-stabilisers off. 350kn, 10000ft
	-1280	-910	1.35	-22.5	-22.4	-13.3	-4.5	
53.6	-3150	-2280	1.38	-54.1	-61.6	-41.8	0.7	
	2660	1870	1.42	45.7	51.0	36.9	-6.5	
57.1	-3760	-3300	1.14	-71.6	-73.1	-71.3	-89.3	Side-slips 200kn 3500ft: Port 'stabs' on, Starboard 'stabs' on
	3860	3470	1.11	75.8	70.6	76.9	93.1	
	-3990	-3470	1.15	-77.5	-78.1	-75.1	-95.3	Port 'stabs' off, Starboard 'stabs' off
	4700	4260	1.10	92.7	87.5	94.8	114.5	
57.2	5490	4300	1.28	97.1	101.3	91.1	-23.9	Rudder kicks 200kn 3500ft: Starboard 'stabs' on, Port 'stabs' on
	-5620	-4420	1.27	-98.8	-107.9	-94.8	19.3	
	6710	5090	1.32	116.3	127.1	105.0	-31.1	Starboard 'stabs' off, Port 'stabs' off
	-5160	-4070	1.27	-91.0	-97.9	-87.3	20.8	
57.3	6730	6330	1.06	135.9	131.7	134.9	113.4	Side-slips 400kn 4500ft: Starboard 'stabs' off, Port 'stabs' off
	-6400	-5860	1.09	-122.4	-123.8	-131.5	-122.8	
	6260	5980	1.05	124.6	121.7	133.3	136.8	Starboard 'stabs' on, Port 'stabs' on
	-5490	-5220	1.05	-109.5	-107.9	-116.5	-118.1	
57.4	12620	9860	1.28	222.9	241.9	204.8	-35.3	Rudder kicks 400kn 4500ft: Starboard 'stabs' off, Port 'stabs' off
	-13040	-10210	1.25	-224.6	-251.9	-218.6	-11.5	
	12200	9610	1.27	213.8	229.6	207.5	-23.9	Starboard 'stabs' on, Port 'stabs' on
	-11720	-9190	1.28	-202.7	-225.6	-196.4	10.4	
57.5	8300	8660	0.96	173.5	164.0	165.3	258.4	Side-slips 550kn 4000ft: Starboard 'stabs' on, Port 'stabs' on
	-7360	-7250	1.01	-143.8	-144.6	-148.4	-207.1	
	6640	6610	1.00	130.8	129.2	131.3	193.6	Starboard 'stabs' off, Port 'stabs' off
	-7820	-7570	1.03	-149.9	-154.0	-149.5	-205.1	
57.6	11920	10020	1.19	215.6	228.1	197.9	66.3	Rudder kicks 500kn 4000ft: Starboard 'stabs' off, Port 'stabs' off
	-12590	-10560	1.19	-221.3	-241.9	-214.8	-105.8	
	12560	10170	1.23	223.5	239.4	202.0	33.1	Starboard 'stabs' on, Port 'stabs' on
	-11520	-9280	1.24	-197.1	-219.6	-186.1	-43.0	
65.1	-8950	-5930	1.51	-141.0	-171.0	-121.0	83.9	Turbulence 550kn, low level
	5020	3800	1.32	87.6	96.0	81.1	-31.1	
	4820	3560	1.36	79.7	92.1	75.4	-29.0	
	7690	5770	1.33	131.9	149.6	117.6	-54.9	
	-4720	-3900	1.21	-89.8	-90.6	-82.8	20.8	
	-3820	-2950	1.30	-70.2	-73.1	-58.3	21.8	
65.2	4800	3330	1.44	78.7	90.4	67.9	-38.9	
	-5380	-4120	1.31	-94.3	-101.3	-83.6	31.6	
	-5630	-4160	1.35	-97.1	-107.3	-86.0	24.4	
	6810	4980	1.37	115.1	129.6	103.5	-52.4	
	-7100	-5080	1.40	-118.5	-135.2	-106.1	51.8	
	5890	4290	1.37	98.6	101.8	87.3	-37.9	
65.3	7360	5220	1.41	121.3	140.0	109.9	-62.1	
	-6710	-4560	1.47	-111.7	-128.7	-93.5	64.8	
	-7740	-5570	1.39	-132.5	-148.1	-117.0	57.0	
	7480	4760	1.57	119.0	144.0	91.1	-84.9	
	-7020	-5390	1.30	-124.7	-135.6	-100.4	24.4	
	6320	4240	1.49	99.9	119.2	92.6	-53.4	
70.1	-6440	-4150	1.55	-108.4	-124.8	-93.9	64.3	Rolling pull-outs, M = 0.9, 35000ft
	10290	6750	1.52	170.1	198.3	155.0	-70.4	
	-6070	-4200	1.44	-105.6	-119.2	-99.0	25.4	
	2810	2060	1.36	51.6	51.7	51.9	-14.0	
70.2	-5820	-3860	1.51	-98.8	-113.3	-91.1	52.4	
	7850	5510	1.43	131.3	150.0	121.3	-16.6	
	-4180	-2890	1.45	-74.1	-81.5	-70.6	25.9	
	1900	1330	1.43	33.2	33.3	29.0	2.1	
70.3	7840	5040	1.55	128.0	151.0	111.0	-65.3	
	-6610	-4660	1.42	-114.0	-127.1	-107.1	24.9	
	4560	3150	1.45	79.2	87.5	72.1	-22.9	
	-2310	-1560	1.48	-40.5	-44.8	-36.5	17.5	
79.1	-3560	-2340	1.52	-57.3	-67.1	-48.8	-20.6	Aileron rolls, one missile 300kn, 12000ft
	2520	1940	1.30	49.4	47.7	39.5	0.0	
	-2960	-2180	1.36	-50.0	-55.2	-47.9	2.1	
	2210	1670	1.32	45.5	42.7	38.6	11.9	
	-1860	-1410	1.32	-32.0	-35.8	-31.4	-1.6	

* Mean of tensile and compressive boom strains.

Table 7

PARAMETERS AVAILABLE FOR RECORDING

Ampex AR200 tape recorder	Transmitter	Range
Shear strain spar 2	Strain gauge bridge	
" " " 3	" " "	
" " " 4	" " "	
" " " 5	" " "	
Shear strain. Rear shear wall	" " "	
Bending strain spar 2	" " "	
" " " 3	" " "	
" " " 4	" " "	
Rate of roll (fine)	EEA gyro FT9	±20deg/s
Rate of roll (coarse)	" " "	±120deg/s
Rate of yaw	" " "	±20deg/s
Lateral g spine	Systron Donner accelerometer 4310	±1g
Lateral g fin	RAE accelerometer type 15	±1½g
Normal g spine	McLaren accelerometer	0 - +6g
Angle of sideslip	Airstream direction sensor	±15deg
Angle of sideslip	Penny and Giles vane	±15deg
Rudder angle	Penny and Giles potentiometer	±13deg
Time base	From CID recorder	½ second pulses
Pilot event	Push button in cockpit	
A1322 recorder		
Indicated airspeed	Munro mirror unit	80 to 750kn
Altitude	Barograph G13	-1000 to +65000ft
Normal g spine	Accelerometer J5030	-3 to +5g
Lateral g spine	Accelerometer J511	±1g
Aileron angle port	Penny and Giles potentiometer	±12deg
Tailplane angle (coarse)	" " " "	+5 to -20deg
Rudder angle (coarse)	" " " "	Full travel
Time base	From CID recorder	½ second pulses
Pilot event	Push button in cockpit	
Strain gauge bridge supply volts	Monitor on strain gauge supply box	0 to 11 volts
CID recorder		
Rate of pitch	EEA gyro FT9	±20deg/s
Rate of yaw	" " "	±20deg/s
Rate of roll (fine)	" " "	±20deg/s
Rate of roll (coarse)	" " "	±120deg/s
Time base	Internal timer	½ second pulses
Pilot event	Push button in cockpit	

SYMBOLS

BM_{root}	fin root bending moment (N m)
B_2, B_3, B_4	strain gauge bridges measuring bending moment in spars 2, 3 and 4 at fin root
M	Mach number
p_s	static pressure (N/m^2)
p_{tot}	total pressure (N/m^2). Equal to $p_s\left[1 + \frac{\gamma - 1}{2} M^2\right]^{\gamma/\gamma-1}$
q	dynamic pressure (N/m^2). Difference between total and static pressures ($p_{tot} - p_s$)
S_{root}	fin root shear force (N)
$S_2 - S_5$, S_{rsw}	strain gauge bridges measuring shear in spars 2 to 5 and rear shear wall at fin root
V_t	true airspeed (m/s)
$\ddot{y}_f$	acceleration sensed by lateral accelerometer at the fin (g). Positive to port
$\ddot{y}_{f_{\mathbb{Q}_L}}$	lateral acceleration at the fuselage horizontal datum line derived by adjusting $\ddot{y}_f$ for the component of roll acceleration due to the offset of the accelerometer from the datum line (g)
$\ddot{y}_{OPT}$	acceleration that would be sensed by lateral accelerometer at optimum fuselage position (g)
$\ddot{y}_s$	acceleration sensed by lateral accelerometer in the spine (g)
$\ddot{y}_{s_{\mathbb{Q}_L}}$	$\ddot{y}_s$ adjusted to fuselage horizontal datum line, as for $\ddot{y}_{f_{\mathbb{Q}_L}}$ above (g)
β	sideslip angle (deg). Positive, slipping to starboard
γ	specific heat ratio for air
ε_{b_2}, ε_{b_3}, ε_{b_4}	longitudinal strains. Average of tensile and compressive in spars 2, 3 and 4 (microstrains)
ε_{S_2} to ε_{S_5}, $\varepsilon_{S_{rsw}}$	shear strains in spars 2 to 5 and rear shear wall (microstrains)
ζ	rudder angle (deg). Positive, rudder to port
$\dot{\phi}$	roll rate (deg/s). Positive, rolling to starboard
$\ddot{\phi}$	roll acceleration (deg/s^2)
$\dot{\psi}$	yaw rate (deg/s). Positive, nose yawing to port
$\ddot{\psi}$	yaw acceleration (deg/s^2)

REFERENCES

No.	Author	Title, etc.
1	H.T. Skopinski W.S. Aiken, Jr. W.B. Huston	Calibration of strain-gauge installations in aircraft structures for the measurement of flight loads. NACA TN 2993 (1953)
2	P.B. Hovell	Operational and load data required for service life estimates for military aircraft and helicopters. RAE Technical Report 74121 (ARC 35855)(1974)
3	P.B. Hovell J.R. Sturgeon	The estimation of the fatigue lives of combat aircraft from operational parametric data. RAE unpublished Material (1976)
4	O. Buxbaum	A relation between measured cg vertical accelerations and the loads of the T-tail of a military airplane. AGARD Report 597, September 1972
5	A.P. Ward	Fatigue load spectra for combat aircraft - their derivation and data requirements. Paper presented at the 8th ICAF Symposium, Lausanne, Switzerland, on 4 June 1975
6	P.B. Hovell D.A. Webber T.A. Roberts	The use of calibrated strain gauges for flight load determination. ARC CP No.1041 (1969)
7	R.G.D. Steel J.H. Torrie	Principles and procedures of statistics. Chapter 14, McGraw Hill Book Co. Inc. (1960)
8	B.R.A. Burns	Flight calibration of the specialities including air-stream direction detector on the Lightning T Mk.4. English Electric Aviation Flight Test Note AFN/P1/207 (1962)

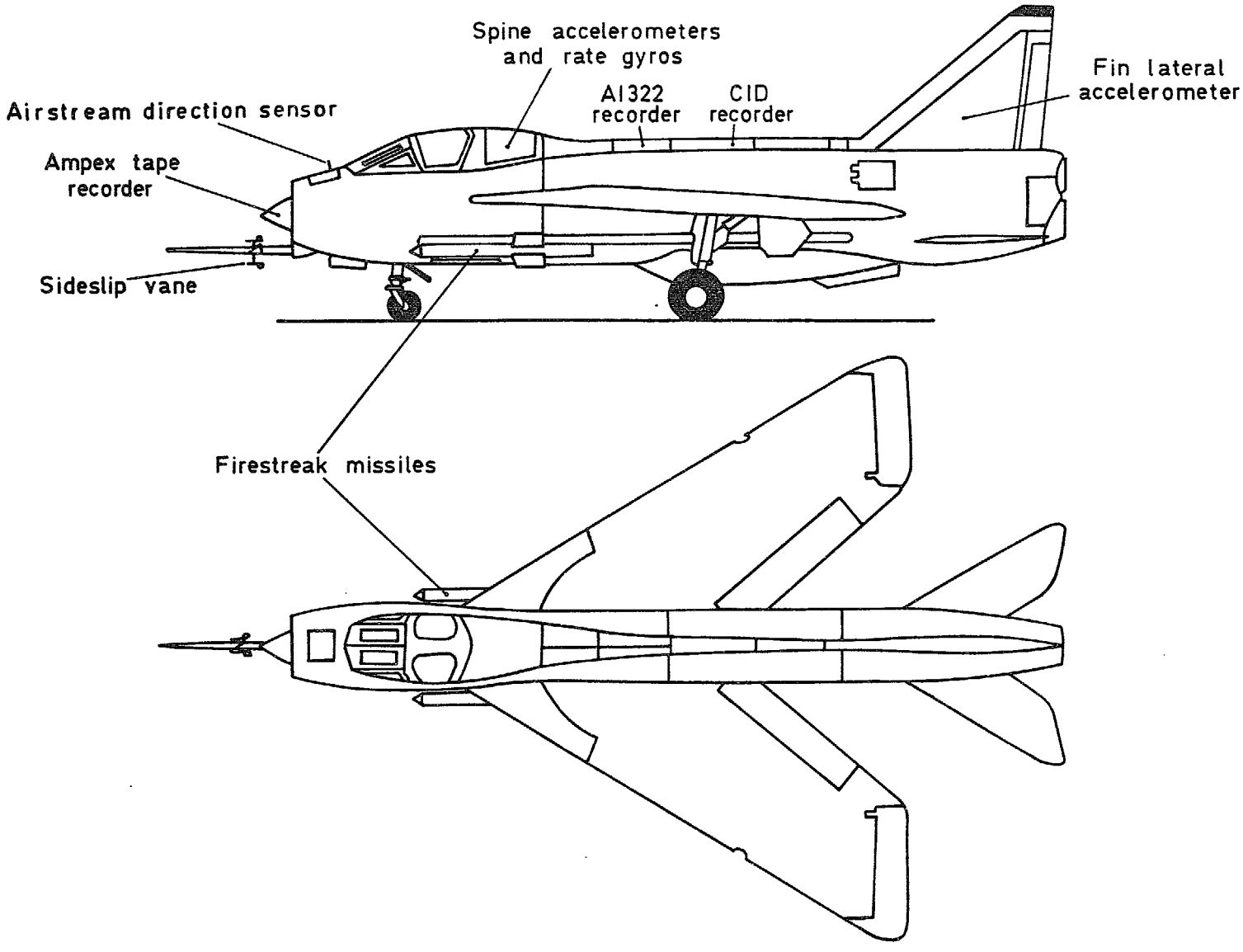

Fig.1 Position of instrumentation on Lightning XM 967

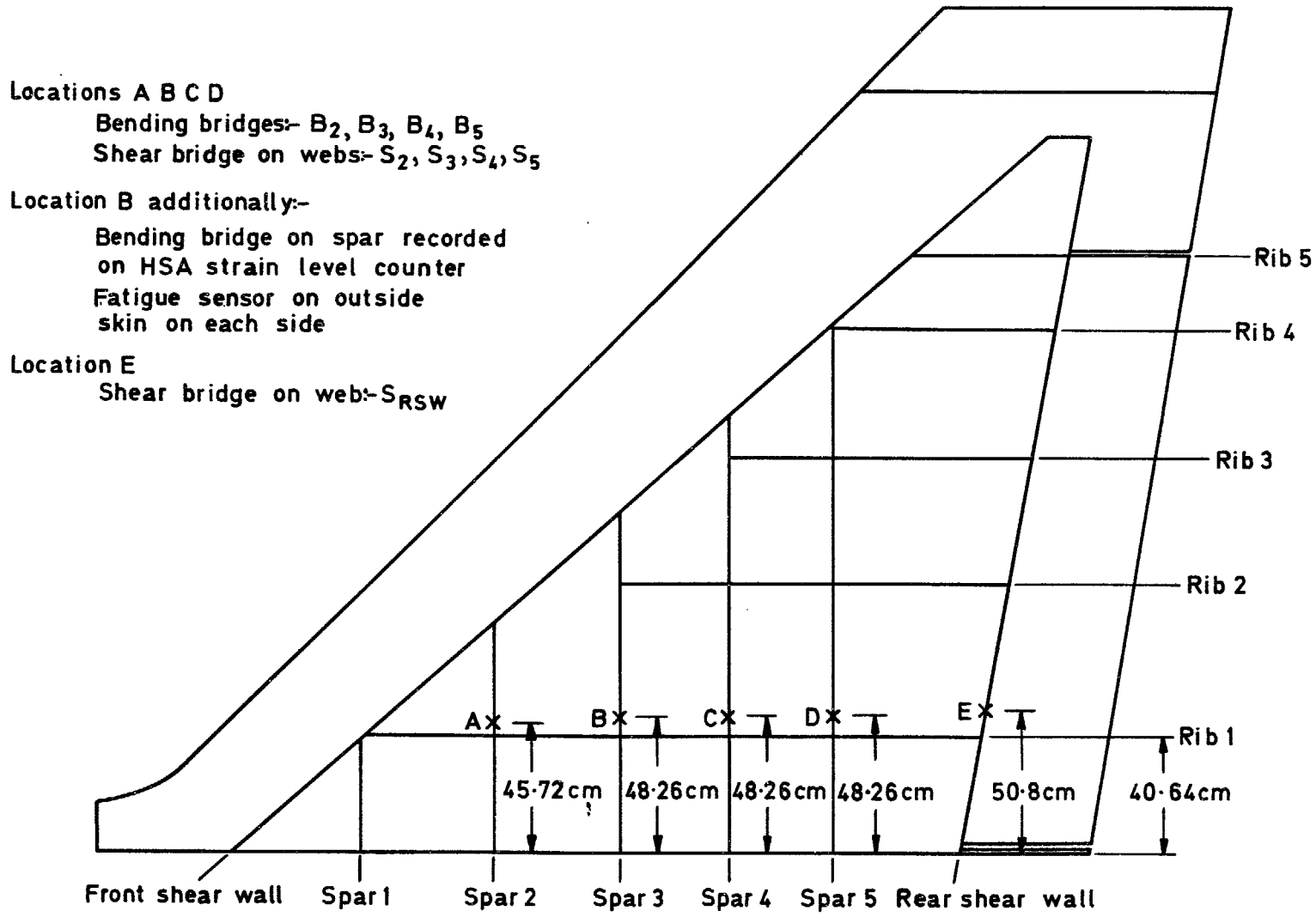

Fig.2 Positions of strain gauges on fin of Lightning XM 967

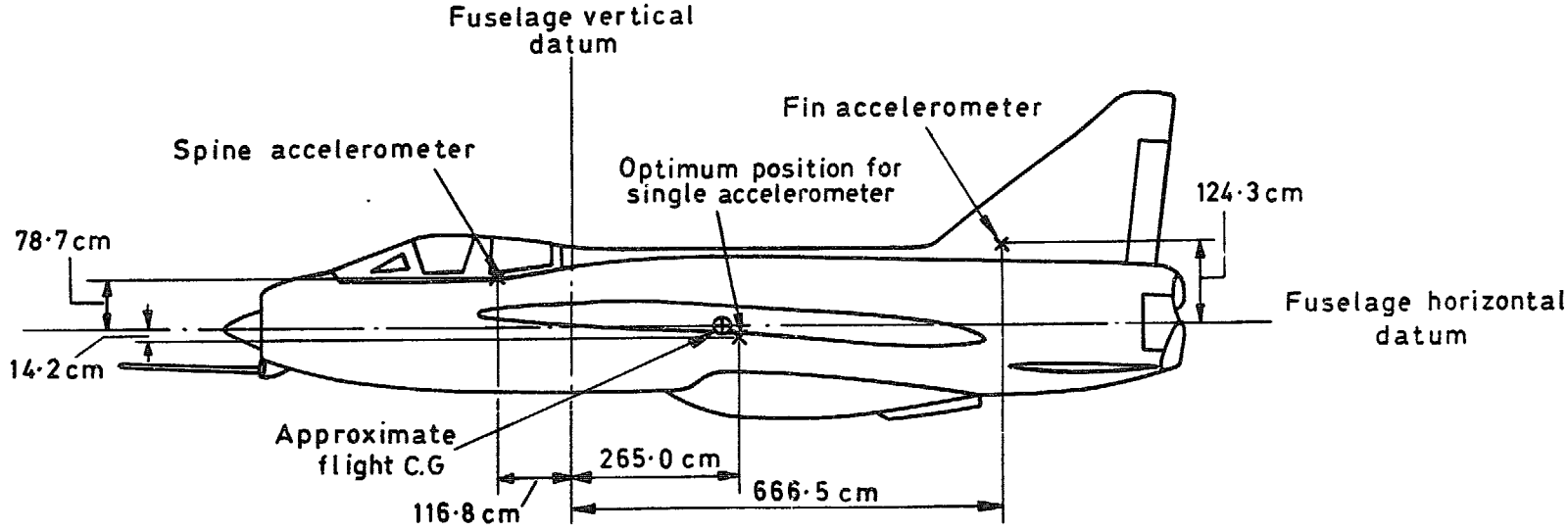

Fig.3 Optimum position for single accelerometer relative to accelerometers fitted

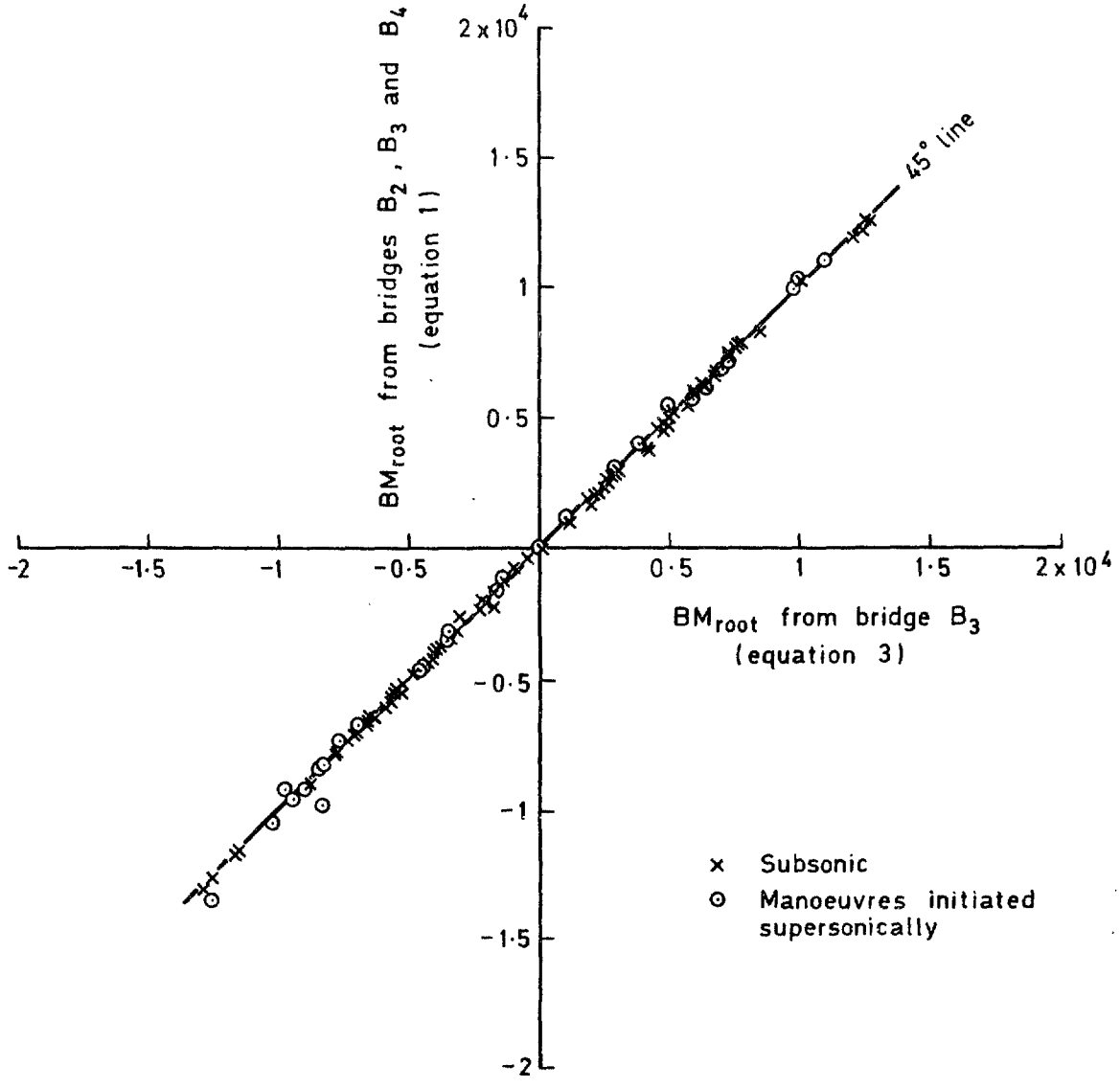

Fig.4 Comparison of fin root bending moments obtained from one and from three strain gauge bridges

Fig 5

$$BM_{root} = 0{\cdot}164\ \dot{\phi}\ \frac{q}{Vt} + 109{\cdot}7\ddot{\phi} + 32300\ddot{y}_F + 31780\ddot{y}_S$$

Total correlation coefficient 0·992

Standard deviation 1300 Nm (12·6% of rms BM_{root})

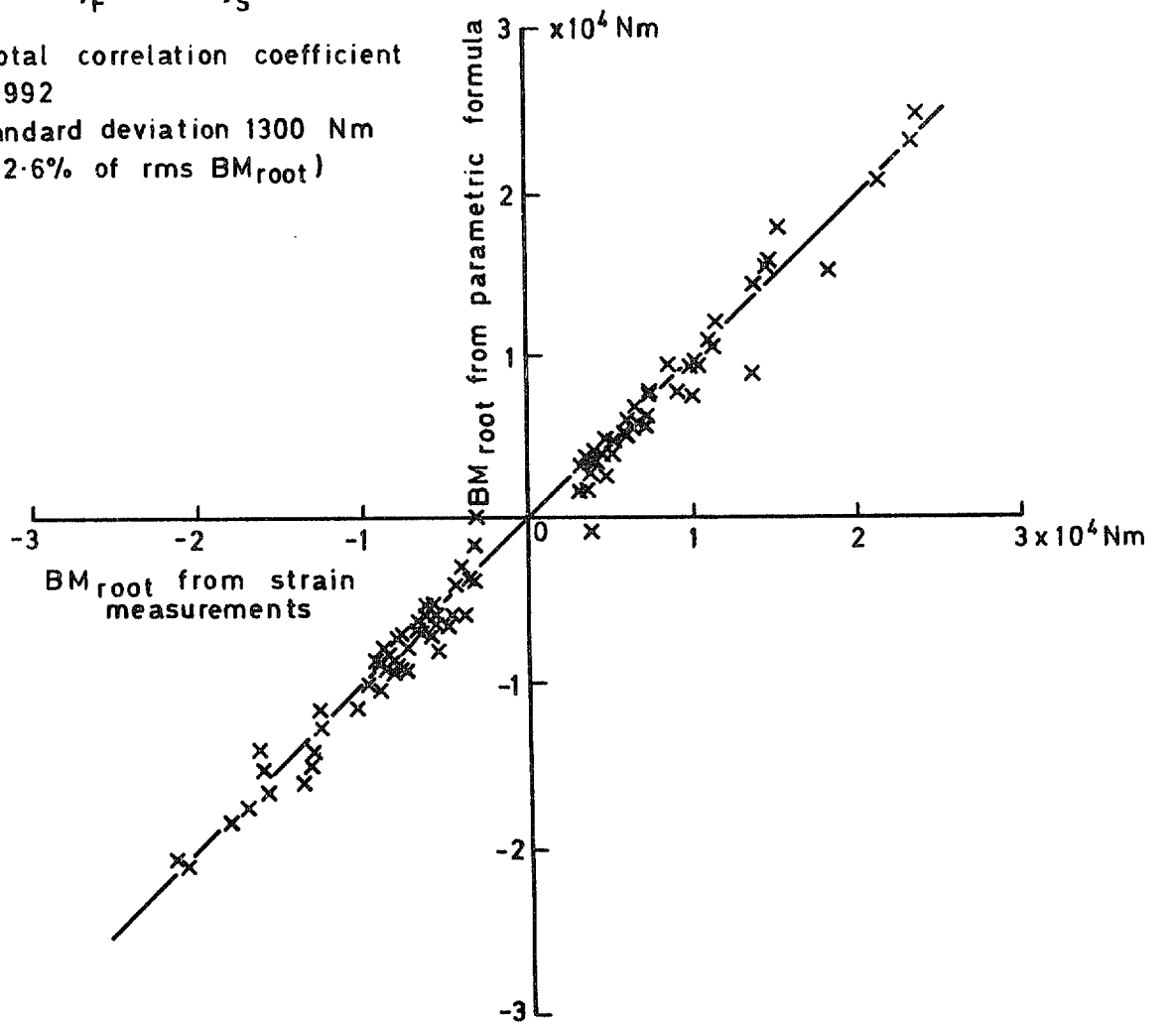

Fig.5 Fit of selected parametric formula

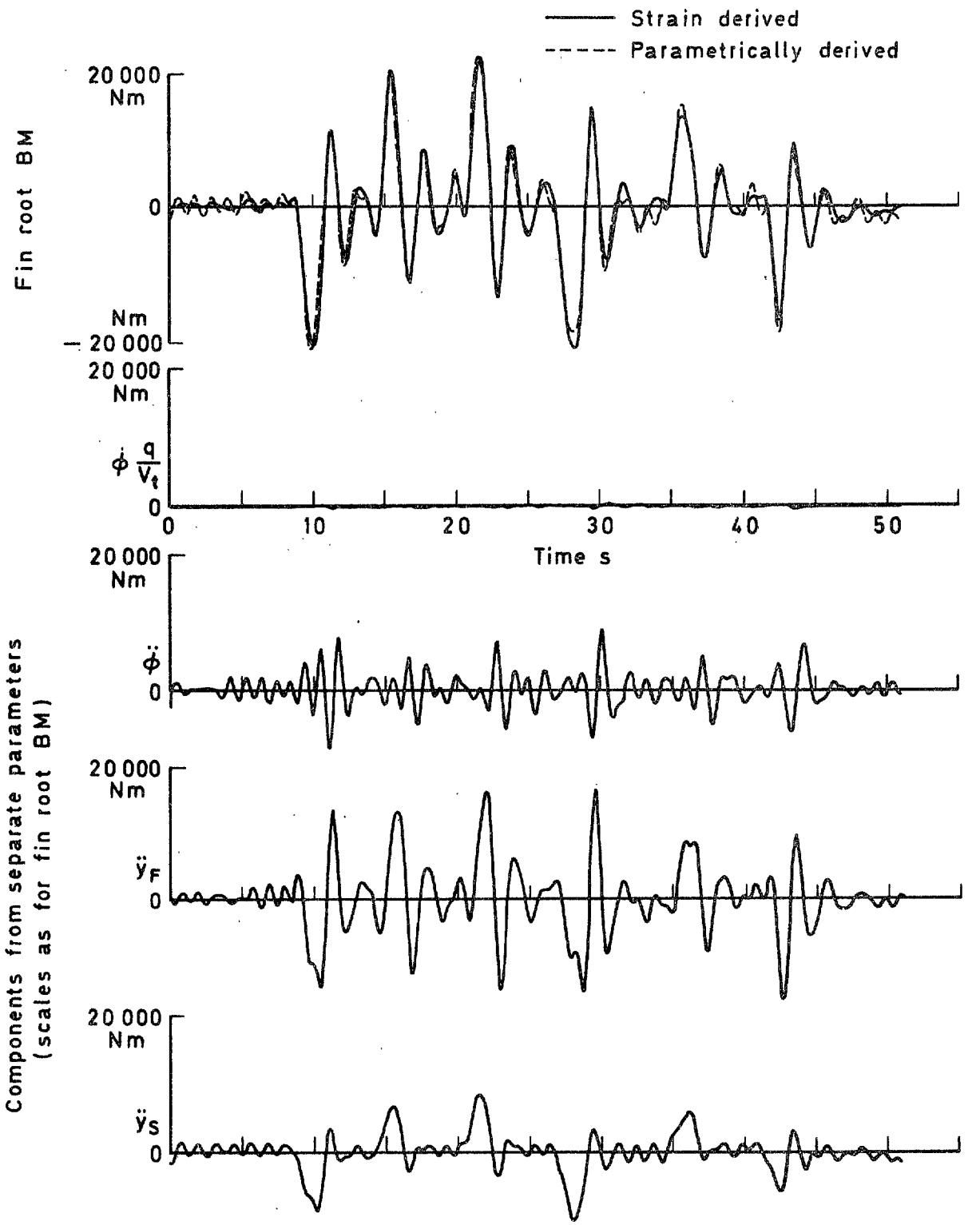

a Flight 137 run 2 Series of yawing manoeuvres
minimum roll 20 000 ft 350 kn

Fig.6 Time histories of parametrically derived and strain derived loads and of separate parametric components — selected formula

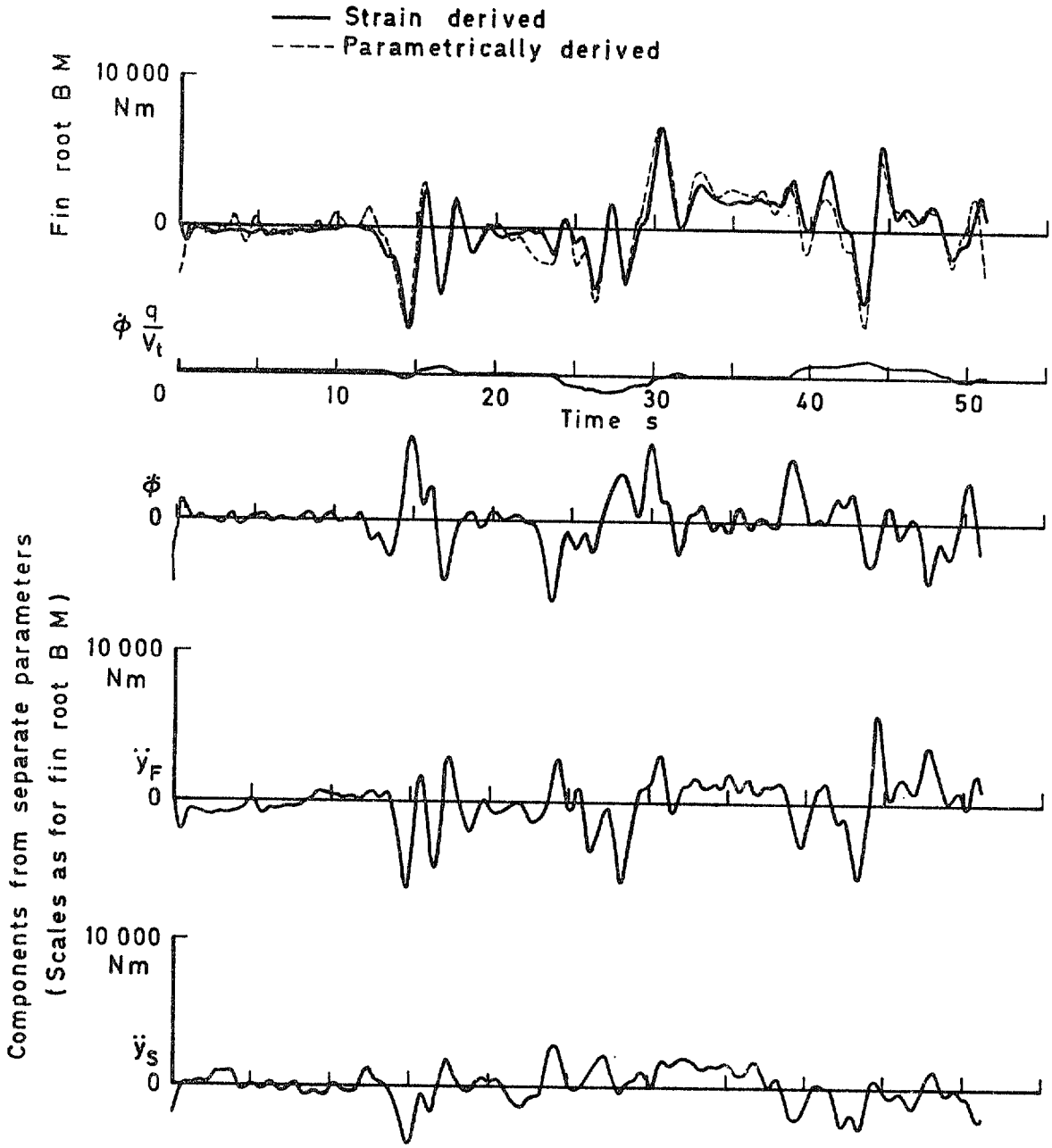

b Flight 137 run 3. Aileron rolls, minimum yawing, 2 port, 1 starboard. 20000 ft 350 kn

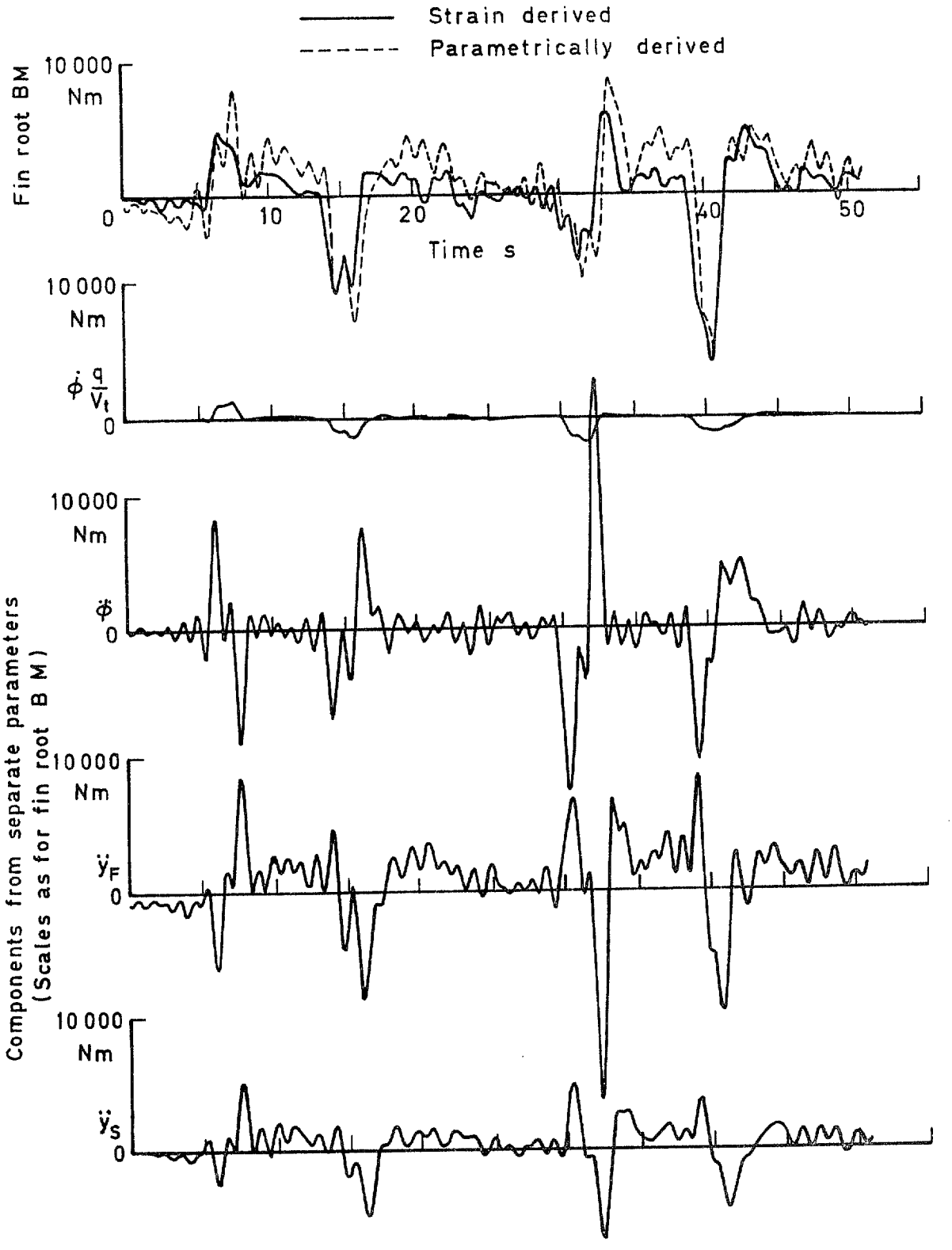

c Flight 153 run 2 Missile breakaway manoeuvre
Initiated 25 000 ft 400 kn

Fig 6 contd

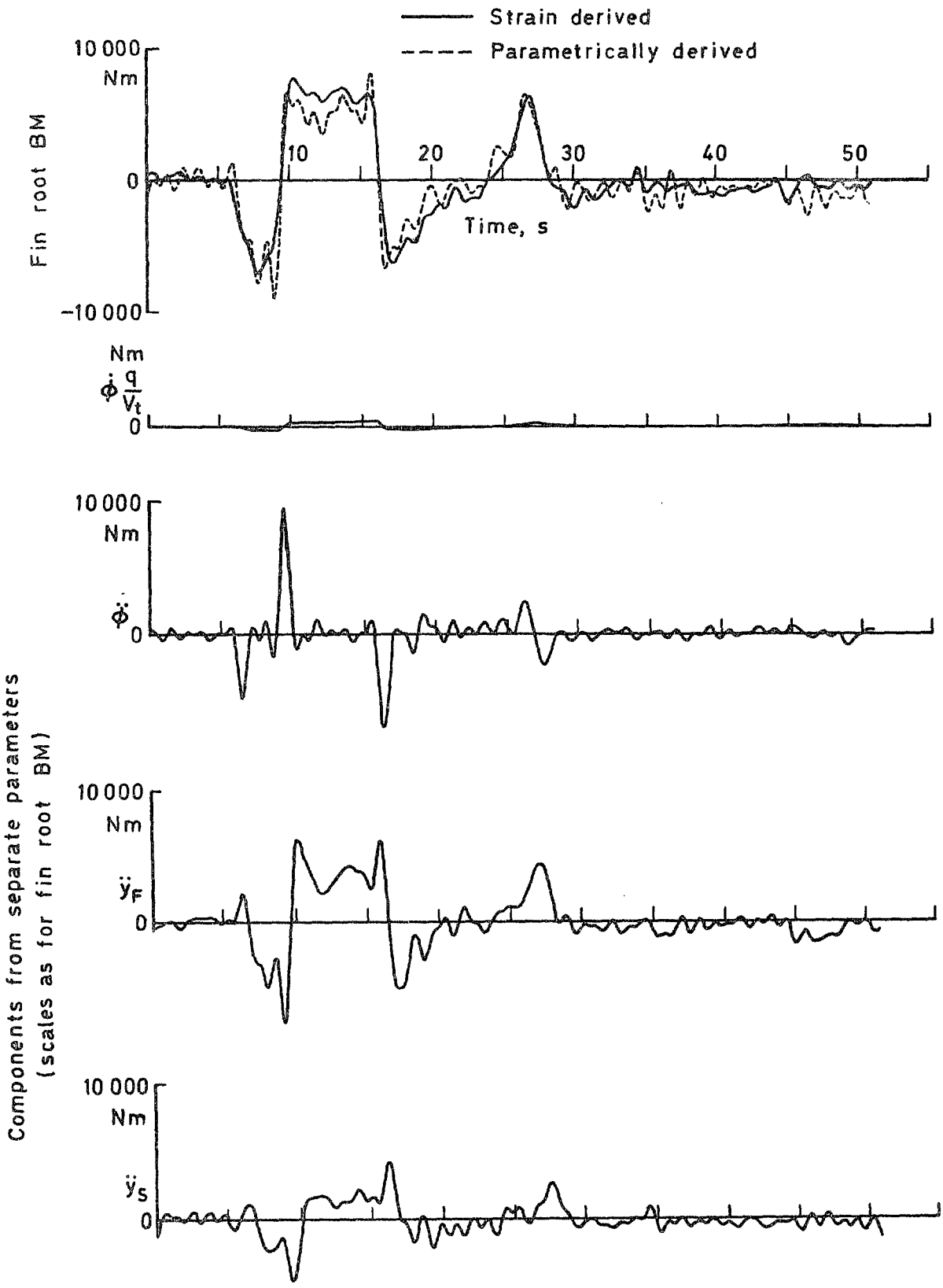

d Flight 148 run 1 180° roll to starboard with stabilisers on 6000 ft. 200 kn

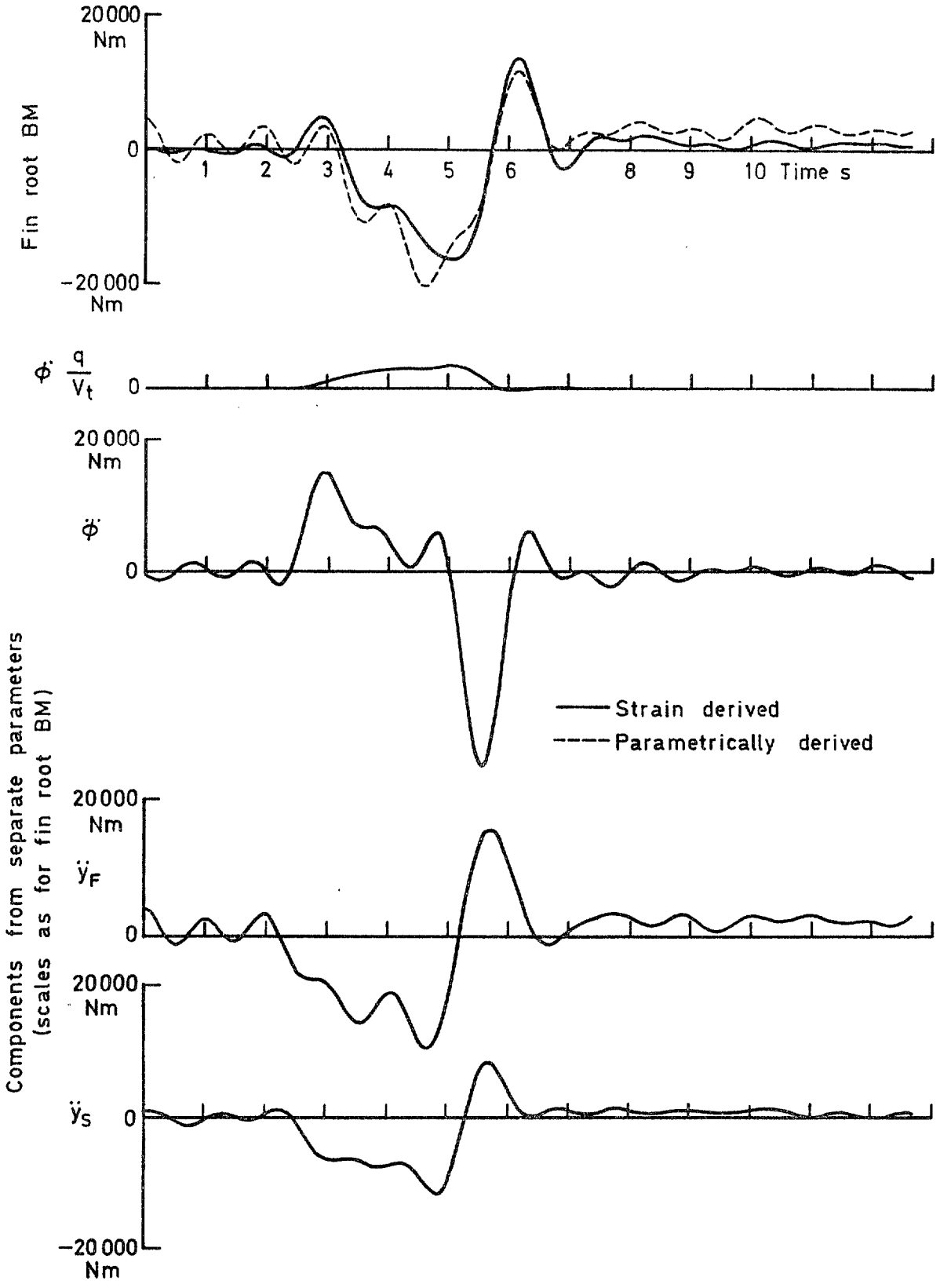

e Flight 148 run 5 Maximum rate rolling, 360° to starboard, stabilisers on. Indicated sideslip 6°port. 6000ft 400kn

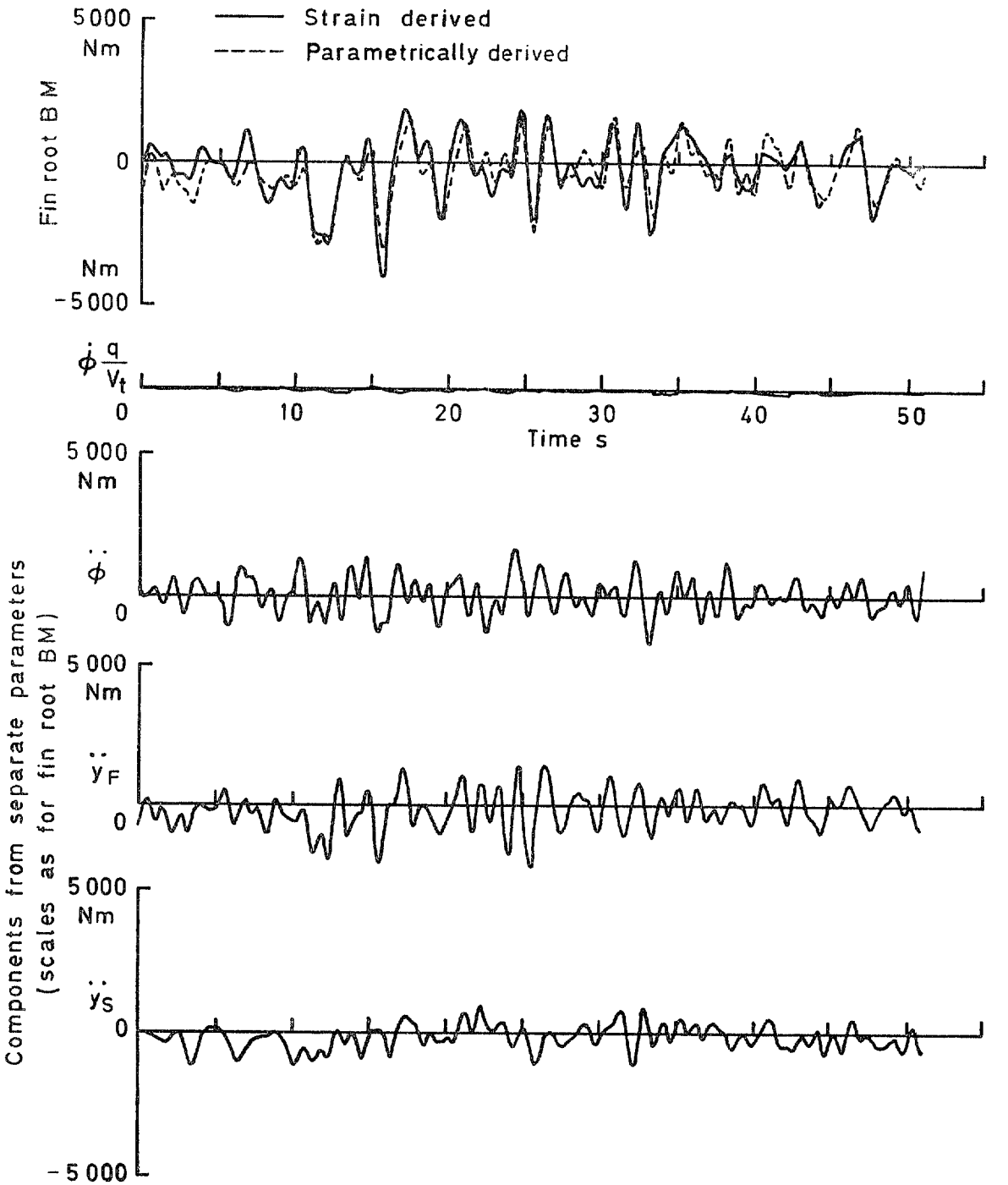

f Flight 158 run 1 Flight refuelling (dry)
29 000 ft, 280 kn

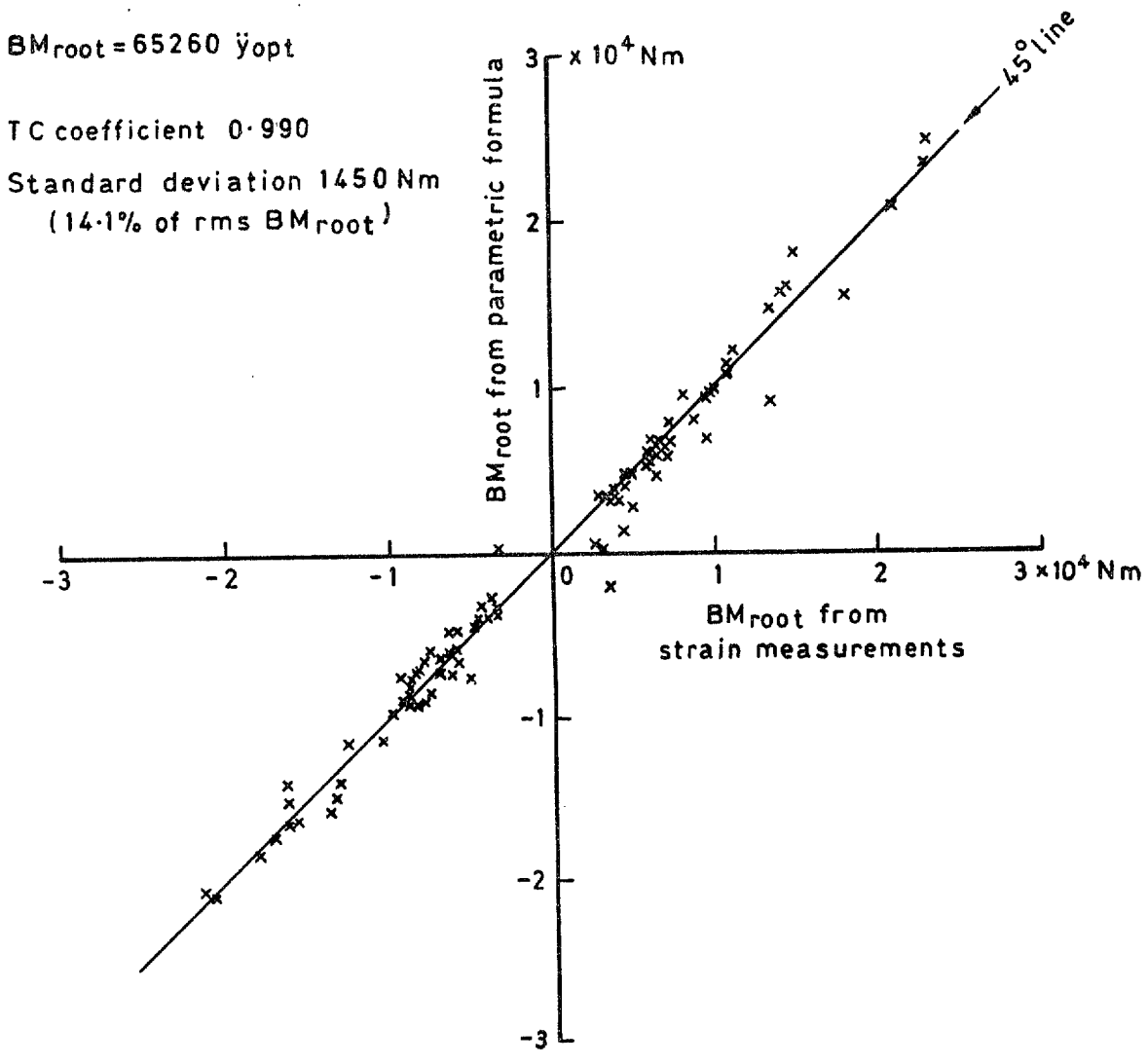

Fig 7 Fit of parametric formula containing the single parameter lateral acceleration near the CG

Fig 8

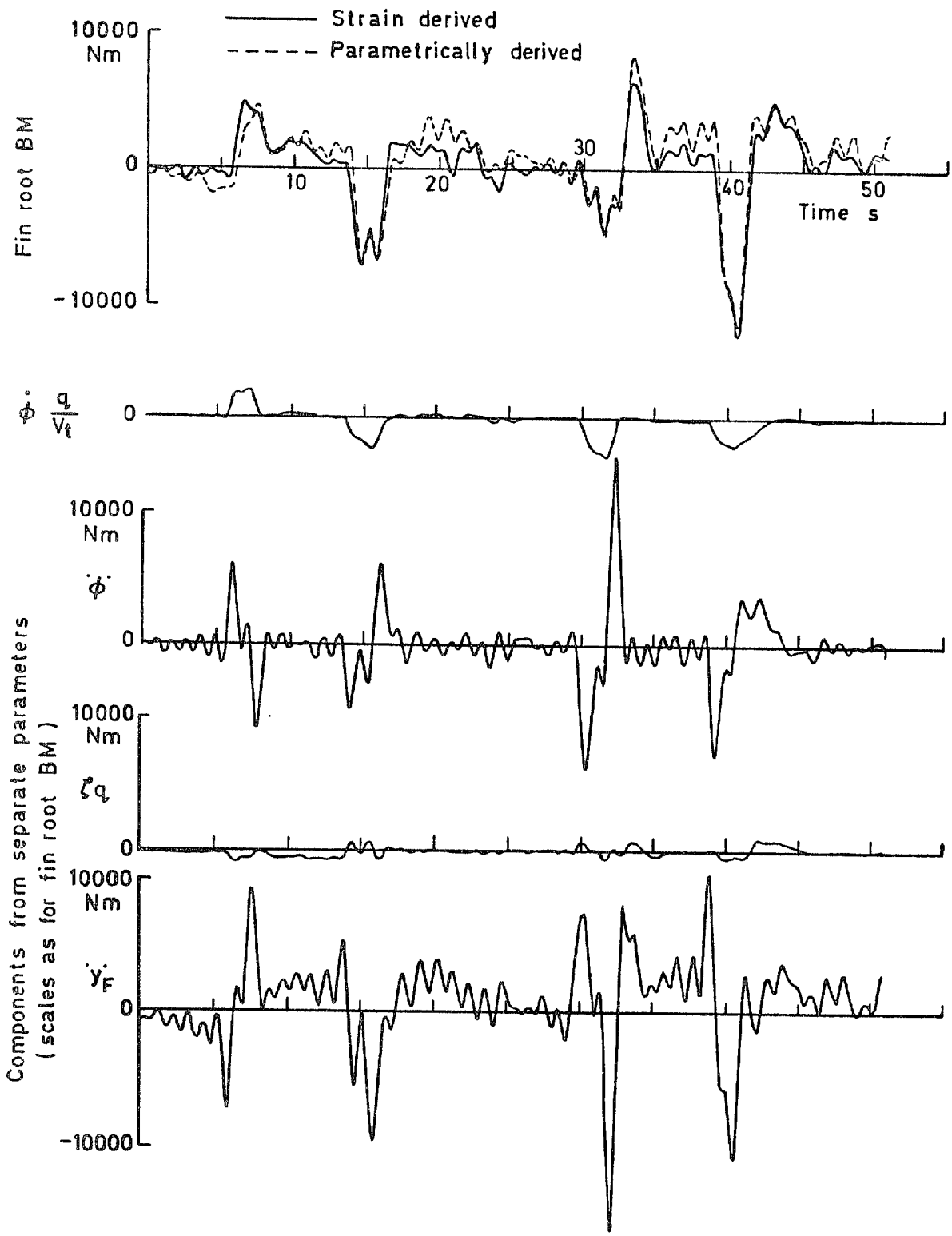

Fig 8 Time histories of parametrically derived and strain derived loads and of separate parametric components — formula with ζ. Flight 153 run 2. Missile breakaway manoeuvre. Initiated 25000 ft 400 kn

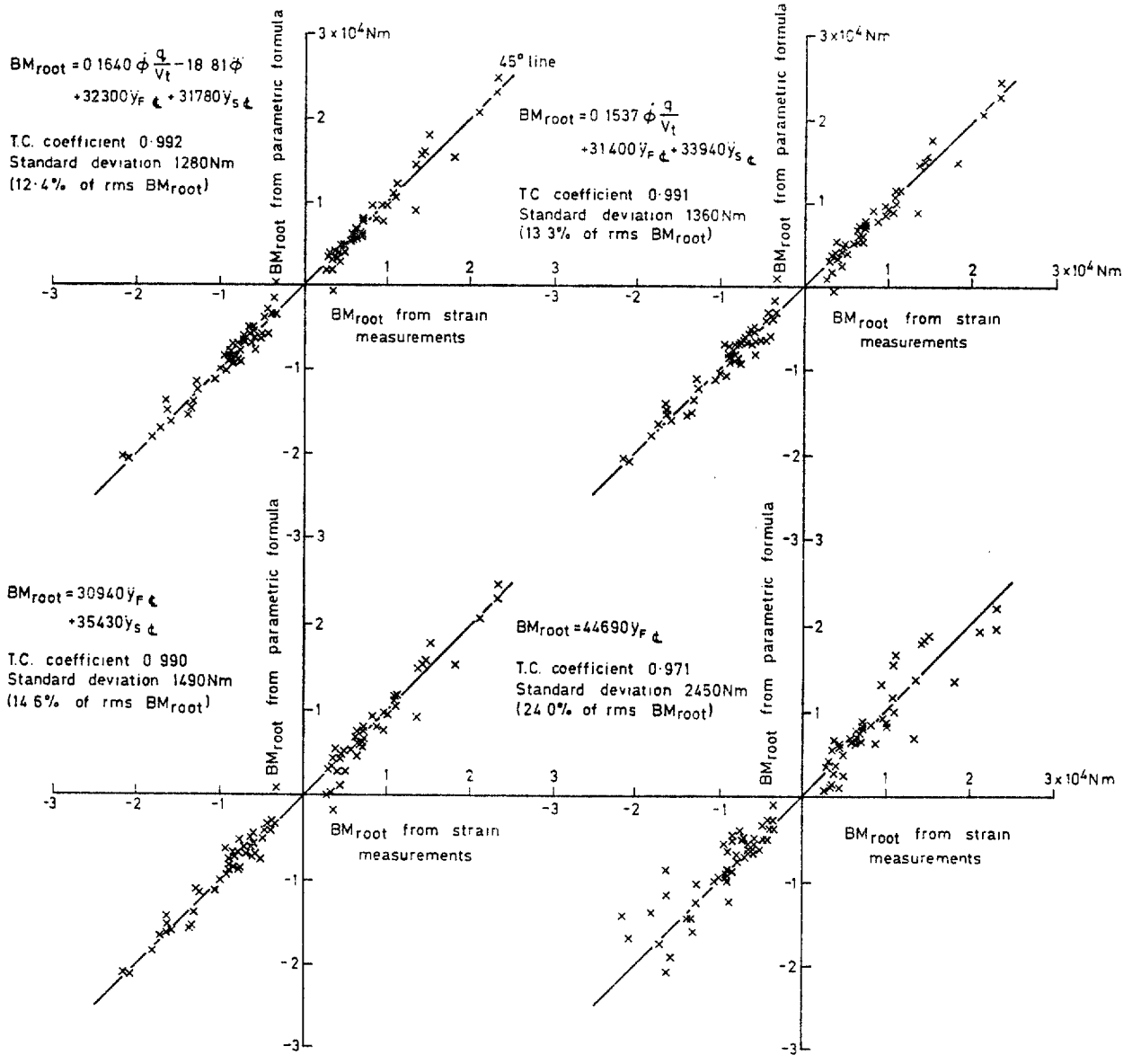

Fig 9 Fit of parametric formulae as parameters are successively discarded (last 4 cases of run 2 of Table 3)

Fig 10

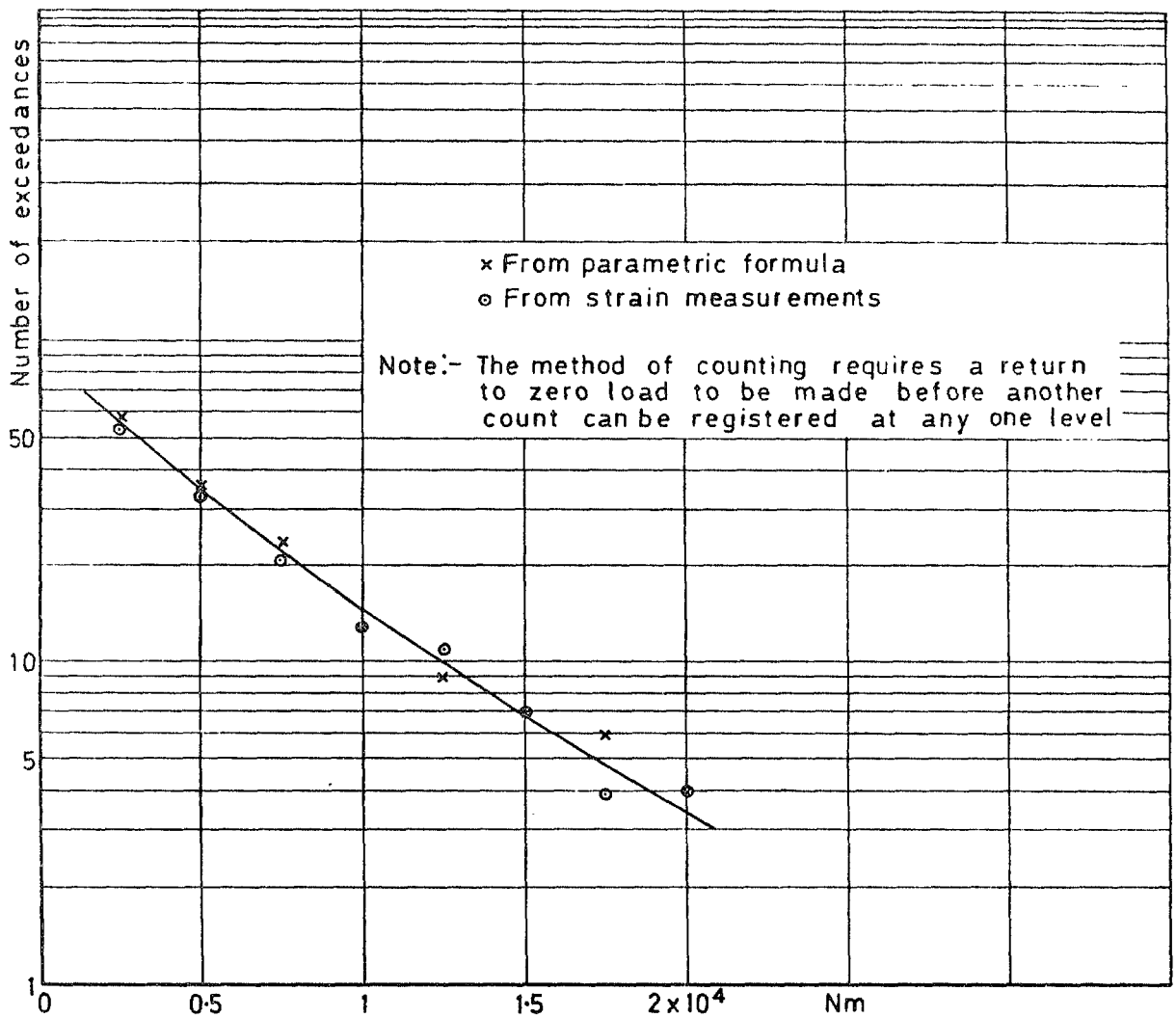

Fig 10 Comparison of load exceedances for parametrically derived and strain derived load histories of Fig 6

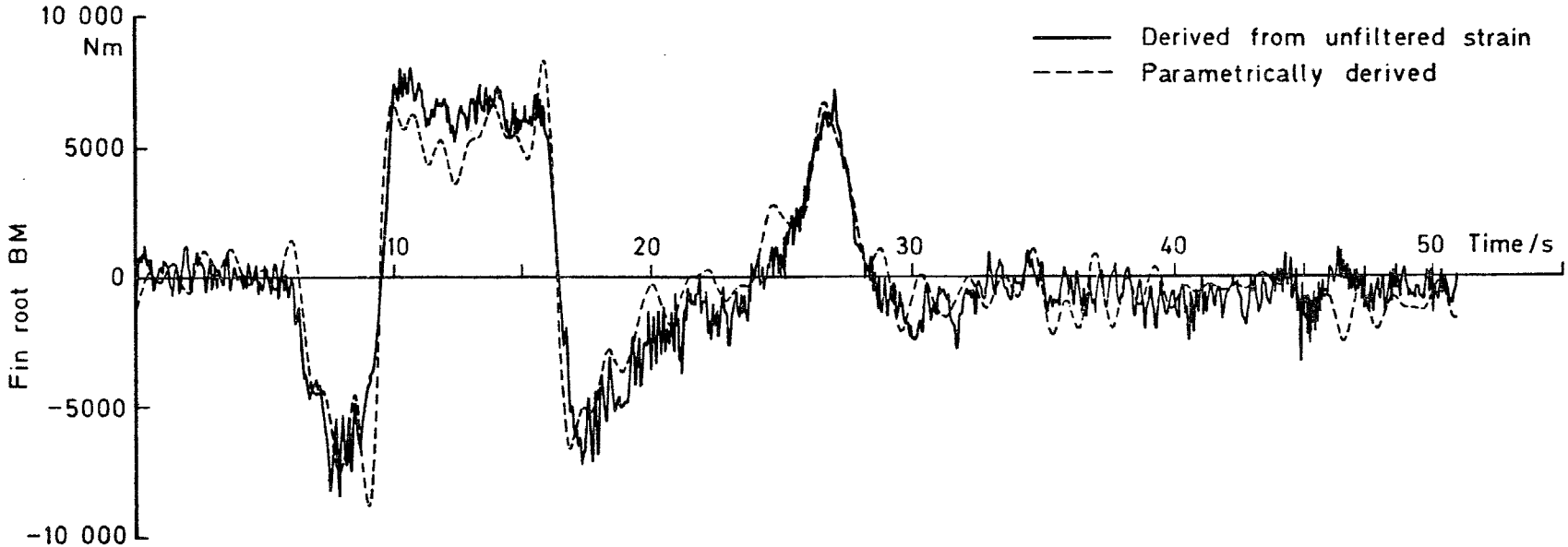

Fig 11 Time histories of parametrically derived load and of load derived from unfiltered strain – selected formula. Flight 148 run 1. 180° roll to starboard with stabilisers on, 6000 ft, 200 kn

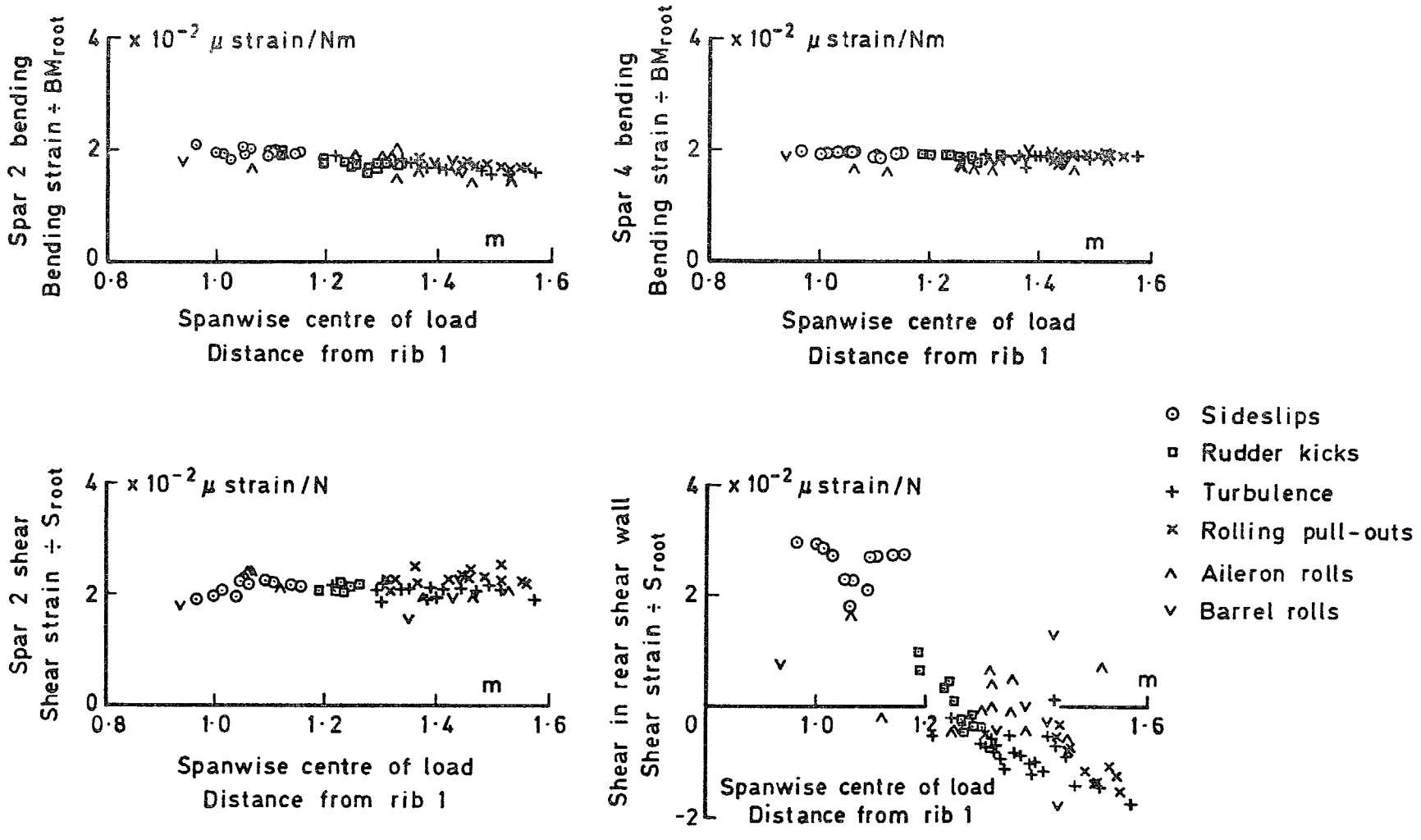

Fig 12 The relation of local spar strains to total fin root load as the spanwise centre of load varies

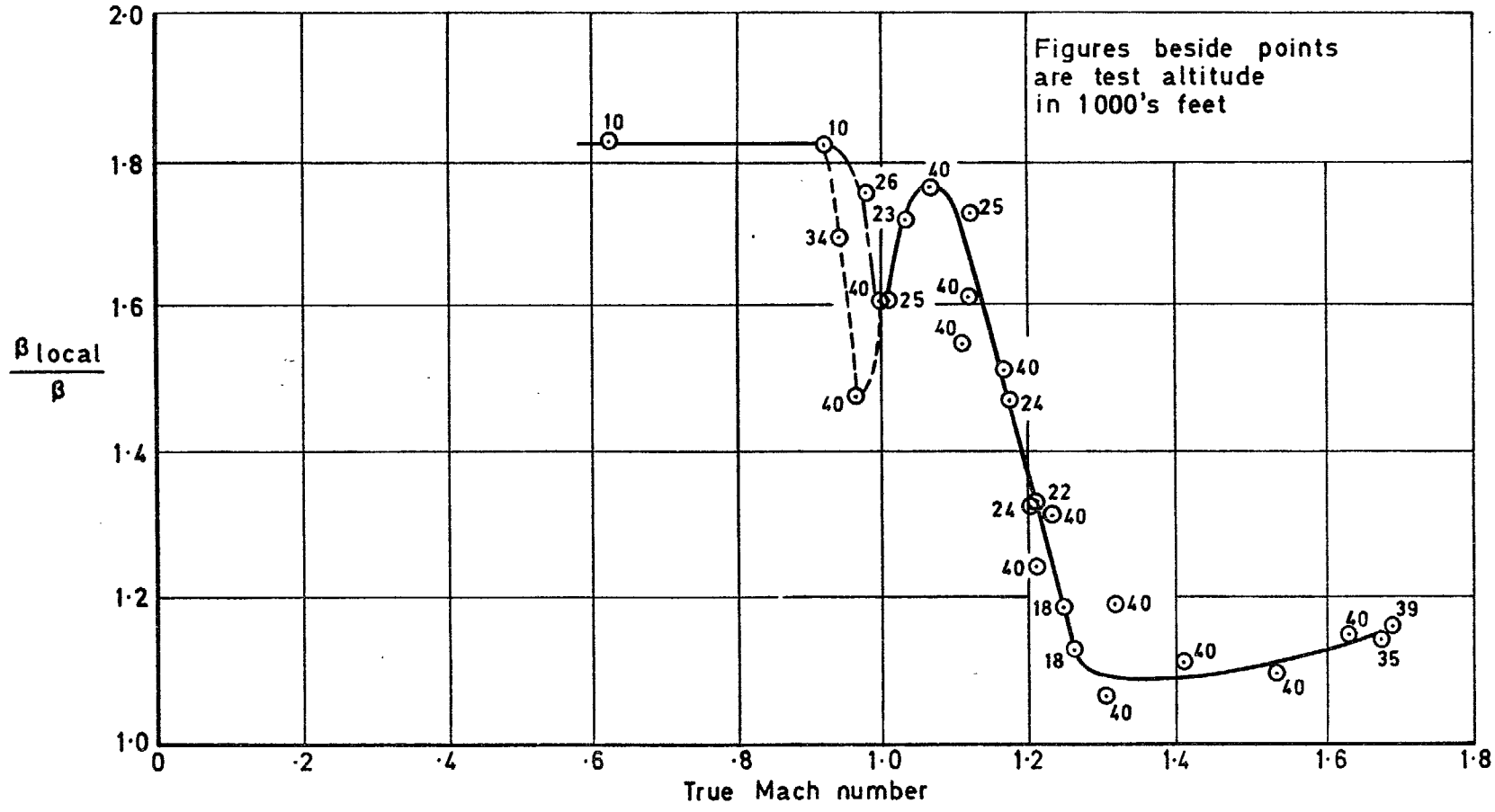

Fig 13 Airstream direction sensor — calibration factor
(Extracted from Ref 8)

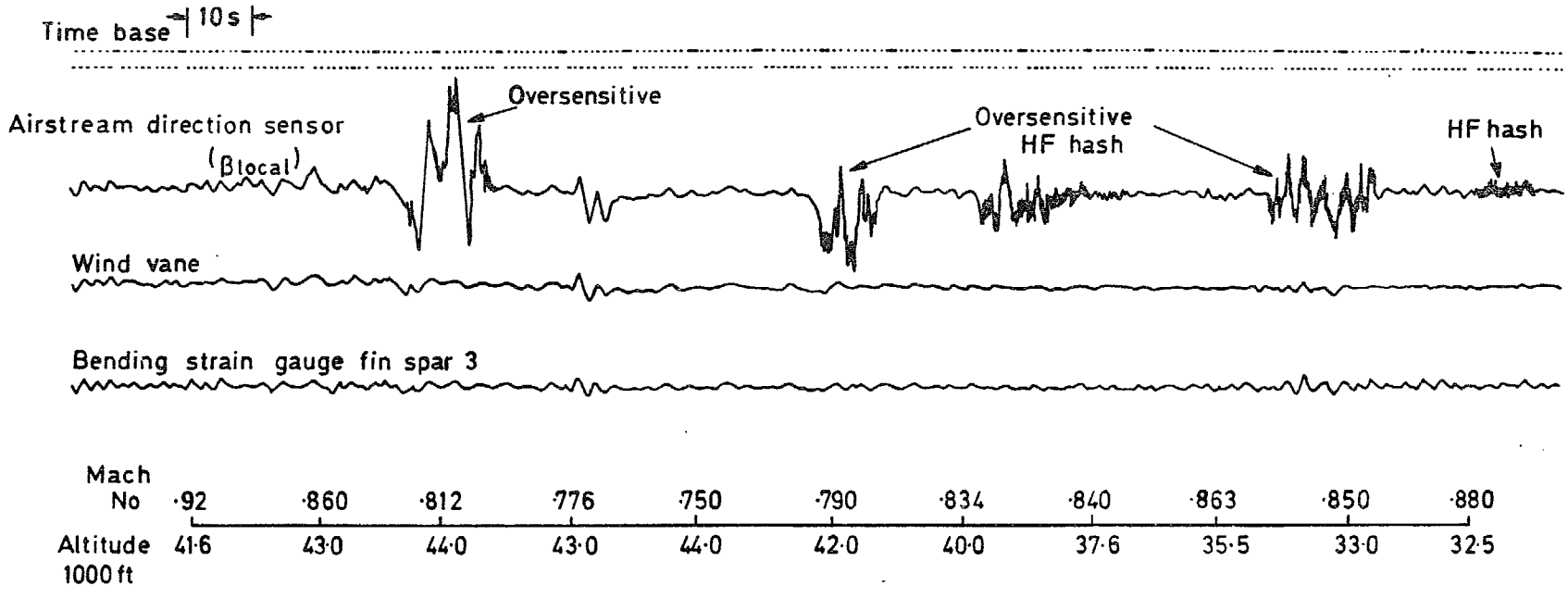

Fig 14a **Malfunctioning of the airstream direction sensor and vane sideslip indicators during descent**

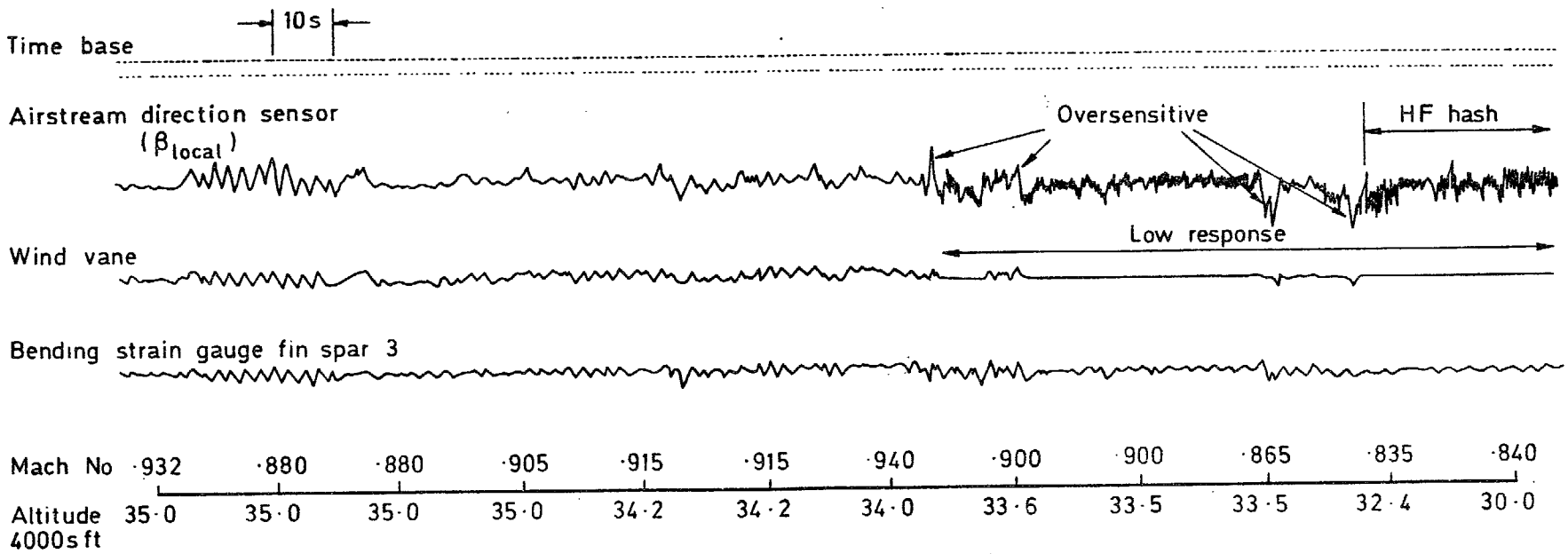

Fig 14b **Malfunctioning of the airstream direction sensor and vane sideslip indicators in transonic flight**

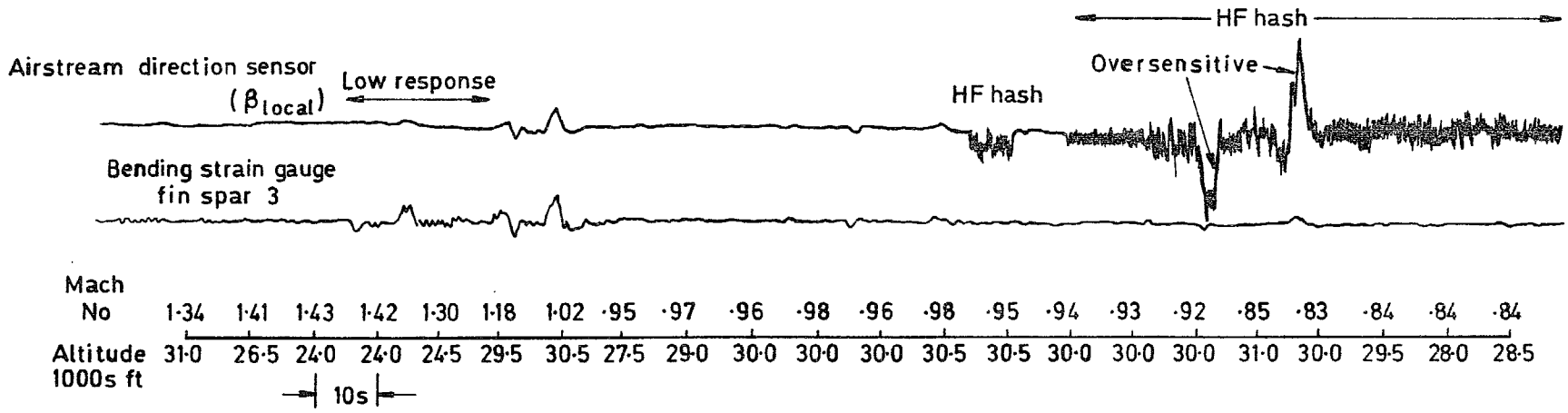

Fig 14c **Malfunctioning of the airstream direction sensor sideslip probe in supersonic manoeuvre and recovery**

Printed in England for Her Majesty's Stationery Office by the Royal Aircraft Establishment, Farnborough. Dd. 587484 K4 8/78.

1978

Published by
HER MAJESTY'S STATIONERY OFFICE

Government Bookshops
49 High Holborn, London WC1V 6HB
13a Castle Street, Edinburgh EH2 3AR
41 The Hayes, Cardiff CF1 1JW
Brazennose Street, Manchester M60 8AS
Southey House, Wine Street, Bristol BS1 2BQ
258 Broad Street, Birmingham B1 2HE
80 Chichester Street, Belfast BT1 4JY

Government Publications are also available through booksellers

R &M No.3824
ISBN 0 11 471157 7